TR 155
6634-1-F

CONSIDERATIONS IN LORAN-C/D RECEIVER DESIGN

By

David L. Mills

COOLEY ELECTRONICS LABORATORY

Department of Electrical Engineering
The University of Michigan
Ann Arbor, Michigan

Lear-Siegler, Inc.
Ann Arbor, Michigan

October 1964

ACKNOWLEDGMENT

Grateful acknowledgment is accorded to Dr. B. F. Barton for assistance and advice in the preparation of this report.

TABLE OF CONTENTS

Section		Page
	ACKNOWLEDGMENT	i
	TABLE OF CONTENTS	ii
	LIST OF ILLUSTRATIONS	iv
	LIST OF TABLES	v
1	INTRODUCTION	1
2	SIGNAL CHARACTERISTICS	2
	2.1 System Pulses	4
	2.2 Pulse Coding	5
3	SIGNAL DESCRIPTION	8
	3.1 Average Power	8
	3.2 Correlation Functions	9
	3.3 Power Spectrum	24
	3.4 Anti-jam Margin	25
4	INTERFERENCE MODEL	26
	4.1 Whiganoi	26
	4.2 Sferics	27
	4.3 Cochannel Signals	29
	4.4 Skywaves	31
5	SIGNAL RECOVERY	34
	5.1 Carrier Phase	35
	5.2 Envelope	37
	5.3 Preprocessing Gating	39
6	SIGNAL PROCESSING	43
	6.1 Crosscorrelation Techniques	43
	6.2 Autocorrelation Techniques	47
	6.3 Comb Filters	52
	6.4 Information Storage in Integration Processes	53

TABLE OF CONTENTS (Cont.)

Section		Page
7	BIBLIOGRAPHY	56
	A. Loran-C/D System Description	57
	B. VLF Propagation and Interference	58
	C. Pulsed-System Detection and Processing	59
	D. General Theory of Detection in Noisy Environments	61

LIST OF ILLUSTRATIONS

Figures		Page
1	Loran-C signals.	3
2	Envelope waveshape.	5
3	Loran-C basic period.	7
4	Single-pulse autocorrelation function.	10
5	Signal power spectrum.	24
6	Sferic time waveform.	27
7	Sferic power spectrum.	28
8	Differential amplitudes on a North Altantic path.	30
9	Multipath skywaves.	31
10	Skywave intensities.	32
11	Predetection gating.	34
12	Detector signal.	35
13	Derived envelope.	38
14	Crosscorrelation detector.	44
15	Synchronous detector.	46
16	Commuted synchronous detector.	46
17	Detector output.	48
18	Matched filter impulse response.	48
19	Matched filter.	50
20	Master-slave matched filter.	51
21	Comb filter.	52

LIST OF TABLES

		Page
1	Pulse coding.	6
2	Loran-C/D correlation functions.	12— 23

1. INTRODUCTION

The Loran-C/D system is a long-range navigation system designed to provide accurate position information throughout the world. The Loran-C system, still under construction, will consist of a number of three- or four-station nets which provide bearing and distance information within a 4000-km service range. The Loran-D system, in the developmental stage, is evidently intended for somewhat smaller ranges but higher precisions and anti-jam capabilities. The two systems are designed to be compatible with each other and to use similar detection, processing, and coordinate-conversion techniques. Present receiving equipment, whether carried by man or installed in air, sea, or land vehicles, is expected to provide accuracies of a few hundred feet throughout the service range.

Both systems use a time-comparison method in which the times-of-arrival of pulse groups transmitted by three or more very-low frequency (vlf) stations are compared to fix hyperbolic lines of position. To achieve inherent system accuracies, these time uncertainties must be reduced to the order of 0.1 μs in correlated and uncorrelated noise environments 20-80 db above the signal. The purpose of this report is to explore detection and processing techniques for the extraction of Loran-C/D signals in such environments.

2. SIGNAL CHARACTERISTICS

The principal advantages of vlf for Loran-C/D operation lie in the small groundwave path losses and the relatively well-understood propagation phenomena (B4, B5).* Currently all Loran-C/D systems are assigned a carrier frequency of 100 kc, which is time-shared among the stations of a net for identification and resolution purposes. Timing information is carried by coded pulse groups which are periodic at intervals in the 30 to 100-ms range.

Each Loran-C net consists of three or more stations up to 1000 km apart, all of which are assigned a unique basic period in the 30 to 100-ms range. One of the stations of the net is designated the master and transmits an identifying code of two groups of eight phase-flipped pulses separated by half the basic period. The other two stations are designated slaves and transmit similar code groups which are phase-locked to the master by off-the-air receivers at the slave sites. The master and its slaves are differentiated by the pulse codes, and the slaves are differentiated from each other by their time sequence relative to the master. Appropriate delays are inserted at the slaves to insure that the three signals do not overlap anywhere in the service area (A1, A2). Figure 1 illustrates the situation. Pulse groups are labeled as either the master or one of its two slaves. The basic

* Symbols within parentheses refer to entries in the Bibliography.

period consists of two half-periods containing identical pulse patterns from all stations except that the phase coding is different. This choice of coding was motivated by considerations of multipath distortion, which will be discussed in Section 4. The amplitudes of the pulse groups from the various stations may differ by as much as 80 db in certain locations in the service area.

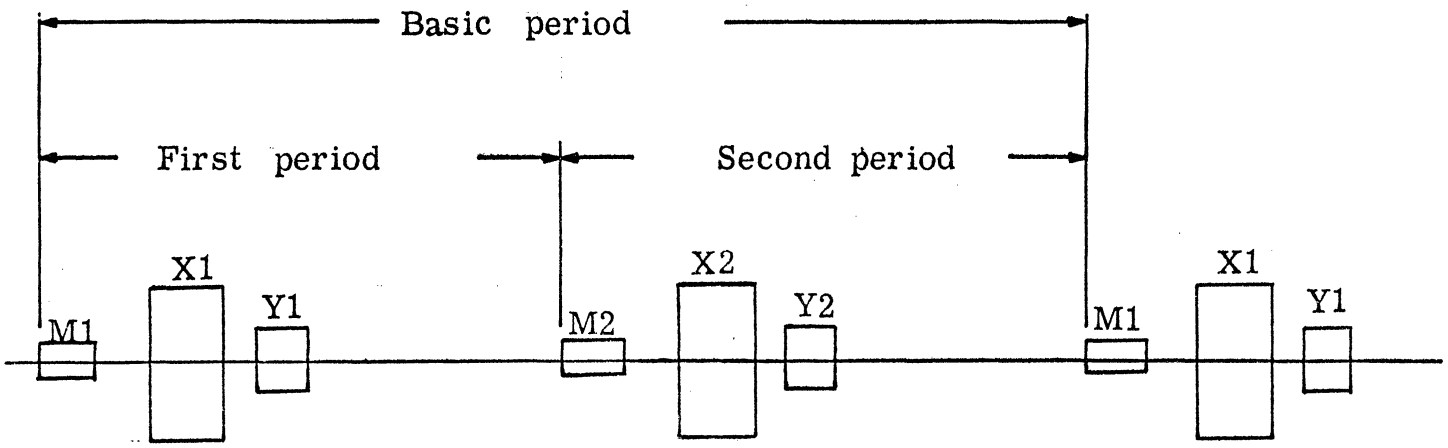

Fig. 1. Loran-C signals.

The Loran-D net is similar to the Loran-C net with respect to the station geometry and carrier frequency. The Loran-D system achieves greater precision through the use of a longer pulse-group code. Twice the number of pulses are transmitted (A9) in a group at twice the pulse rate. However, the basic period is double that for Loran-C since the phase coding of the inserted pulses alternates in successive pulse groups. Since the systems differ only in this manner, and are compatible, most of the

succeeding discussion will deal with the Loran-C system; the extension of the results to the Loran-D system is readily apparent.

Doppler frequency shifts up to 0.2 cps are experienced in high-speed airborne equipment at speeds of 1200 knots. A local clock synchronized to the carrier of each station is necessary for tracking purposes; measuring the frequency differences between the clocks provides a source of velocity information. The three clocks considerably complicate the receiver and, furthermore, place a limit on the processing integration time unless there is sufficient additional information about aircraft velocity, heading, and maneuvers.

2.1 System Pulses

Each pulse group consists of eight system pulses which are identical except possibly for carrier phase. The envelope waveshape has been tailored to yield the fastest risetime consistent with the radiated spectrum width limitations of 20 kc. For reasons which will be demonstrated later, only the first 30 μs of this envelope (3 carrier cycles) are useful for time-of-arrival measurements.

The restrictions upon bandwidth have led to an envelope waveshape which has a third-cycle amplitude of 0.45 for a peak eighth-cycle amplitude of 1.0. The carrier power at the third-cycle is called the sampling-point power and is used in the definition of the S/N ratios of the system. Present transmitters radiate an effective power of one megawatt at the sampling point (A4).

A pulse shape which has been empirically found to meet these requirements satisfactorily has the normalized envelope function $t^2 e^{2-2t}$ (see Fig. 2).

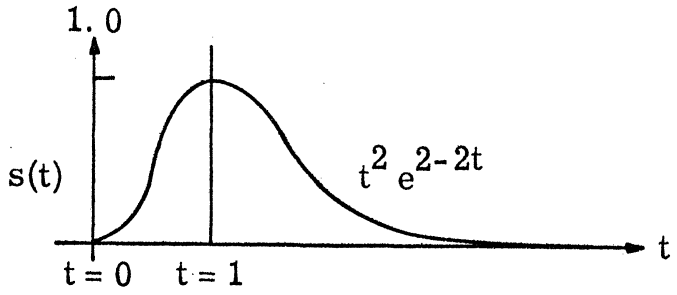

Fig. 2. Envelope waveshape.

This pulse has a peak power of 1.0, which affords a convenient normalization. In the Loran-C case the t = 1 point corresponds to t = 80 μs on the system pulse. At the sampling point t = 30 μs, the amplitude of the pulse is about 0.45.

2.2 Pulse Coding

Table 1 shows the transmitted pulse codes for the Loran-C and Loran-D systems (A6, A9). The basic period is divided by halves in the Loran-C system and by quarters in the Loran-D system, and the indicated code used in each subperiod. These particular codes were chosen for their autocorrelation and crosscorrelation properties in the elimination of skywave interference and implementation of acquisition and tracking processes. Within each pulse group the individual pulse envelope is as

discussed above. The pulses are spaced at intervals of a millisecond in the Loran-C case and at intervals of a half-millisecond in the Loran-D.

Station	System	Subperiod	Coding
MASTER	C	1	++--+-+-
"	C	2	+--++++
SLAVE	C	1	++++++-+
"	C	2	+-+-+---
MASTER	D	1	+++++-+--++-++--+
"	D	2	++-+-++-+-+-+++-
"	D	3	+-+----++---++--
"	D	4	+-----++++++++-++
SLAVE	D	1	+++-++++++------++
"	D	2	++--++-++++++-+--
"	D	3	+-+++-+-++-+-++-
"	D	4	+--++---+-+----+

Table 1. Pulse coding.

Figure 3 is an example of a Loran-C signal showing the relationship between the basic period, the subperiods, and the pulse groups. The times shown are typical. An inspection will varify that if the even-numbered Loran-D pulses are removed, the resulting signal has the same coding as the Loran-C signal.

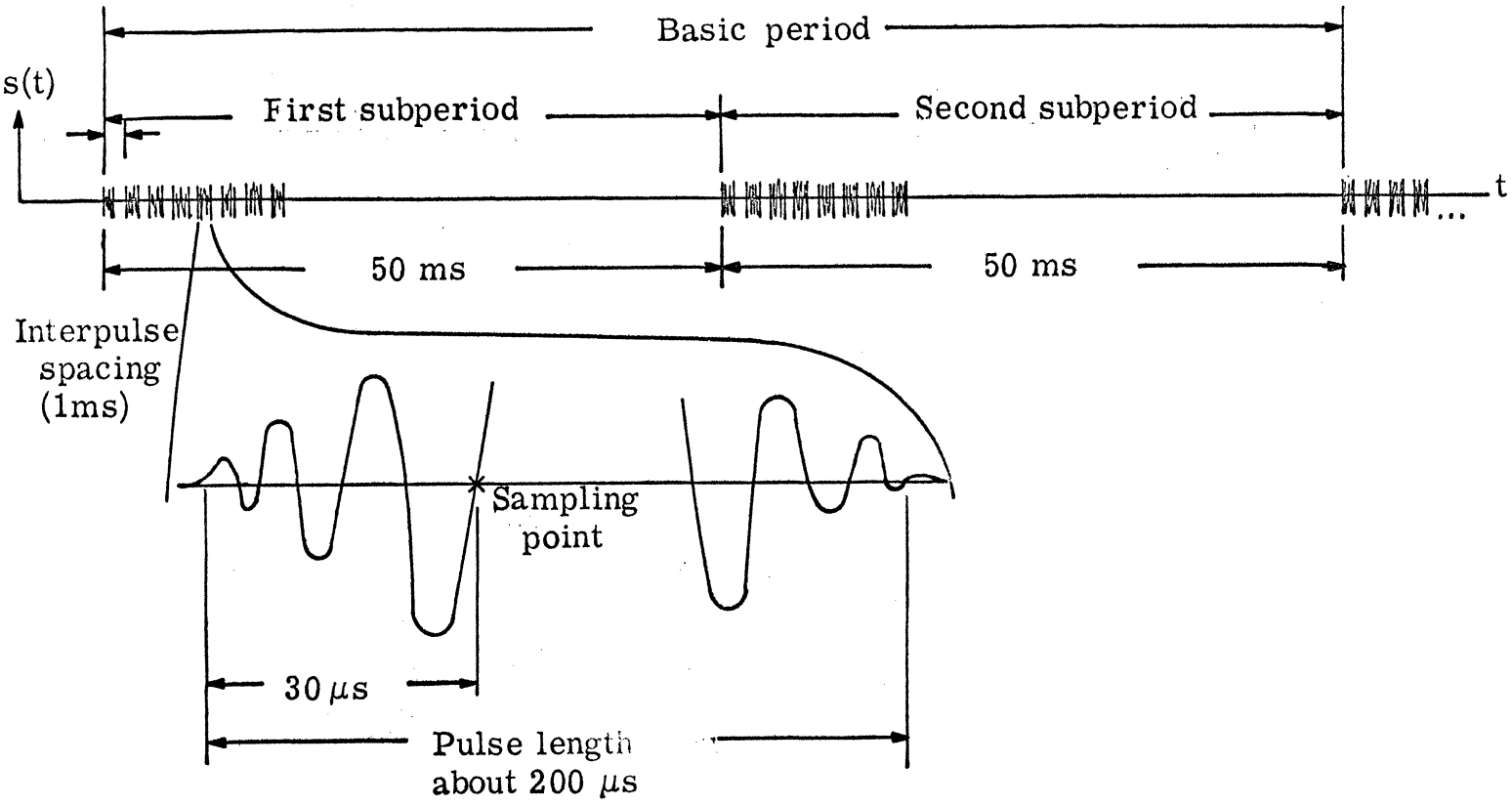

Fig. 3. Loran-C basic period.

3. SIGNAL DESCRIPTION

The Loran-C/D signal can be described in several ways, each appropriate for certain detection processes (discussed in Section 5). This section will specify the following parameters for the Loran-C signal: average and peak powers, autocorrelation and crosscorrelation functions, power spectrum, and anti-jam margin. Attention will be confined to the Loran-C case; to extend the results to the Loran-D case involves merely changing certain constants and the correlation functions, which are easily computed.

3.1 Average Power

Since each pulse of the group is of the form $t^2 e^{2-2t}$, and the $t = 1$ point of this envelope corresponds with the 80-μs point of the pulse, an interpulse spacing of 1000 μs would correspond to a value of t equal to 12.5 (see Fig. 2). The peak power of each pulse has been normalized to one watt; the average power of the pulse group is

$$P_{AV} = \frac{n}{T} \int_0^T s^2(t)\, dt = \frac{n}{T} \int_0^T t^4 e^{4-4t}\, dt$$

$$\cong \frac{3n e^4}{128T} \quad \text{for} \quad T > 10 \ .$$

For example, in a basic period of 100 ms, there are 16 pulses. The average power is then

$$P_{AV} = \frac{3 \times 16 \times e^4}{128 \times 12.5 \times 100} = .0162 \text{ watt.}$$

The sampling point power at t = 30 μs is

$$P_s = (0.45)^2 = .2025 \text{ watt .}$$

Since the signal energy specification involves only the sampling-point power, the peak and average powers have only minor importance except in transmitter design. For example, a transmitter with a sampling-point power of a megawatt must carry a peak-power rating of four megawatts, yet the average power is only about 64 kilowatts.

3.2 Correlation Functions

The correlation functions for the Loran-C/D signal can be readily computed. The autocorrelation function takes the form

$$\psi(\tau) = \int_{-\infty}^{\infty} s(t)\, s(t+\tau)\, dt \quad .$$

We are interested primarily in the envelope of this function, which will appear vaguely like a modulated 100-kc signal. We will evaluate the resulting integral by first calculating the autocorrelation function for a single pulse and then showing how the complete function can be constructed by superposition using the pulse coding.

The system pulse is described by (see preceding section)

$$s(t) = t^2 e^{2-2t} \qquad (0 \leq t < \tau) .$$

We have normalized the time dimension so that the peak occurs at t = 1. The autocorrelation function is

$$\psi(\tau) = \int_0^T t^2 e^{2-2t} (t+\tau)^2 e^{2-2(t+\tau)} \, dt$$

$$= \frac{e^{4-2\tau}}{32} \left(\frac{3}{4} + \frac{3}{4}\tau + \tau^2 \right) \quad (\tau \geq 0) \; .$$

Taking advantage of the fact that $\psi(\tau)$ is an even function of τ, we can sketch the envelope as shown in Fig. 4.

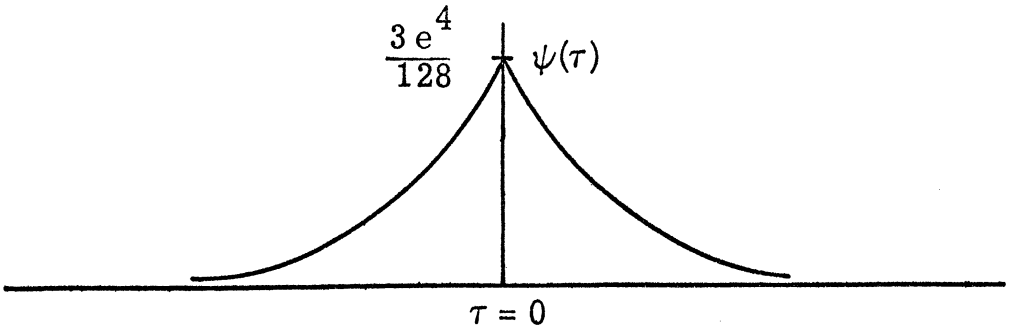

Fig. 4. Single-pulse autocorrelation function.

The important thing about this envelope, from the standpoint of time-of-arrival determination, is that the autocorrelation function be small at time shifts equal to the spacing between pulses (1 ms in Loran-C, 500 μs in Loran-D). In practice, the pulse coding itself helps the situation, and the autocorrelation function can be approximated by a triangle of height $\frac{3e^4}{128}$ and base width of perhaps $\tau = 2$.

The complete autocorrelation function may be constructed by first

scaling the above function so that t = 80 μs corresponds to τ = 1, and then forming the proper correlation peaks by considering the pulse coding.

The Loran-C pulse code for both the master and the slaves has been chosen so the $\psi(\tau)$ vanishes for time shifts of odd multiples of the period between pulses (1 ms). The remaining even-numbered correlation peaks (assuming the principal peak at τ = 0 is 16) are shown in Table 2. Each number in the table represents the scaling to be applied to the above function, which, when filled in with the carrier, yields the actual autocorrelation function.

As we will demonstrate in Section 5, considerable acquisition time can be saved by using autocorrelation techniques (matched filtering). These techniques are practical only when the amplitudes of the subsidiary peaks of the autocorrelation function (at time shifts of other than zero) are small relative to the central peak (at a time shift of zero). In the Loran-C case the subsidiary peaks are at least 12 db down, and are down considerably further in the Loran-D case.

The crosscorrelation function between the master and the slaves may be constructed in a manner similar to the autocorrelation function. It is defined as

$$\phi(\tau) = \int_{-\infty}^{\infty} x(t)\, m(t+\tau)\, dt \quad ,$$

where x(t) is the slave signal and m(t) is the master. The function is

```
$COPIES(30)                                          004845   10/12/64     10 38 19.7 AM
$COMPILE MAD,EXECUTE,DUMP                            LORAN001

MAD (24 SEP 1964 VERSION) PROGRAM LISTING ... ... ...

            CORRELATION FUNCTIONS FOR LORAN C/D (LEAR-SIEGLER 6624)

            NORMAL MODE IS INTEGER                                          *001
            DIMENSION X(16),Y(16),Z(32)                                     *002
            VECTOR VALUES CARD=$C3,16I2*$                                   *003
            VECTOR VALUES LINE=$C4,32I4*$                                   *004
            PRINT COMMENT $1CORRELATION FUNCTIONS FOR LORAN C/D SYSTEMS$    *005
            PRINT COMMENT $OLEAR-SIEGLER (ORA 6624)$                        *006
START       PRINT COMMENT $-INPUT WAVEFORMS$                                *007
            ZERO.(Z(1)...Z(32))                                             *008
            THROUGH LAB.FOR K=1,1,K.G.4                                     *009
            READ FORMAT CARD,ID,X(0)...X(15)                                *010
            PRINT FORMAT LINE,ID,RS.6.V.$ 00000$,X(0)...X(15)               *011
            READ FORMAT CARD,ID,Y(0)...Y(15)                                *012
            PRINT FORMAT LINE,ID,RS.6.V.$ 00000$,Y(0)...Y(15)               *013
            THROUGH LAB.FOR I=-16,1,I.G.16                                  *014
            THROUGH LAB,FOR J=0,1,J.G.15                                    *015
LAB         WHENEVER J+I.GE.0.AND.J+I.LE.15,Z(16+I)=Z(16+I)+X(J)*Y(J+I)     *016
            PRINT COMMENT $OCORRELATION FUNCTION$                           *017
            PRINT FORMAT LINE,$ N$,I(=-15,1,I.G.15,I)                       *018
            PRINT FORMAT LINE,$ Z$,Z(1)...Z(31)                             *019
            TRANSFER TO START                                               *020
            END OF PROGRAM                                                  *021
```

```
MAD PROGRAM,TYPE 10 SEP 1964   (ALL NUMBERS ARE OCTAL)

 NO. OF LOCATIONS 00360 TRA VECTOR SIZE   00005       TRA VECTOR STARTS 00000   ENTRY PT. 00134   ERASABLE STARTS 77777

VARIABLE STORAGE (A=ARRAY,C=COMMON,E=ERASABLE,DIGIT=MODE)
     CARD    00010 A 1        J       00013   1       LAB     00005   4       START   00006   4       Y       00060 A 1
     ID      00011   1        K       00014   1       LINE    00016 A 1       X       00037 A 1       Z       00121 A 1
     I       00012   1

FUNCTION DICTIONARY
     .RCOMT 00000   1        .PRINT 00001   1        .READ   00002   1       SYSTEM 00003   1        ZERO    00004   1

ABSOLUTE CONSTANTS
00122 -207160606060     00123 -204560606060     00124 +000000000017     00125 +000000000000     00126 +000000000020
00127 -200000000000     00130 +000000000006     00131 +000000000004     00132 +000000000001     00133 +233000000000

STATEMENT DICTIONARY
00006 TXL -300161000154
```

$DATA 004845 10/12/64 10 38 30.6 AM

```
MAR
     SCARDS 00000*     SPEEK  00000*     SYSTEM 00000*     ERROR  00000*     SKIP6  00000*     SPRINT 00000*
     (RSCM) 10060      (MAIN) 10000      .IOH   10360*     DFDP   14532*     DFMP   14532*     DPFAD  14571*
     DPFDP  14571*     DPFMP  14571*     DPFSB  14571*     .ERR   14713*     .03311 15001*     .PRINT 15016*
     .READ  15102*     .RCONT 15247*     .EXIT  15266*     ZERO   15360*     (PROG) 15414      (SUBT) 73317
     (ERAS) 77741
EXECUTION BEGINS WITH ROUTINE      (MAIN)
62325 LOCS. CAN BE SAFELY USED IN EXPANDING PROG. (OCTAL)
55703 LOCS. CAN BE SAFELY USED IN EXPANDING PROG. (OCTAL)   BEFORE FULL CORE LOADING PROCEDURE IS USED
```

CORRELATION FUNCTIONS FOR LORAN C/D SYSTEMS

LEAR-SIEGLER (LORA 6624)

INPUT WAVEFORMS

CM1	1	0	1	0	-1	0	-1	0	1	0	-1	0	1	0	-1	0
CM1	1	0	1	0	-1	0	-1	0	1	0	-1	0	1	0	-1	0
CM2	1	0	-1	0	-1	0	1	0	1	0	1	0	1	0	1	0
CM2	1	0	-1	0	-1	0	1	0	1	0	1	0	1	0	1	0
CM1	1	0	1	0	-1	0	-1	0	1	0	-1	0	1	0	-1	0
CM1	1	0	1	0	-1	0	-1	0	1	0	-1	0	1	0	-1	0
CM2	1	0	-1	0	-1	0	1	0	1	0	1	0	1	0	1	0
CM2	1	0	-1	0	-1	0	1	0	1	0	1	0	1	0	1	0

CORRELATION FUNCTION

N	-15	-14	-13	-12	-11	-10	-9	-8	-7	-6	-5	-4	-3	-2	-1	-0	1	2	3	4	5	6	7	8	9	10	11	12	13	14	15
Z	0	-0	0	0	0	0	0	-0	0	-0	0	-0	0	-0	0	32	0	-0	0	-0	0	-0	0	-0	0	0	0	0	0	-0	0

INPUT WAVEFORMS

CM1	1	0	1	0	-1	0	-1	0	1	0	-1	0	1	0	-1	0
CM2	1	0	-1	0	-1	0	1	0	1	0	1	0	1	0	1	0
CM2	1	0	-1	0	-1	0	1	0	1	0	1	0	1	0	1	0
CM1	1	0	1	0	-1	0	-1	0	1	0	-1	0	1	0	-1	0
CM1	1	0	1	0	-1	0	-1	0	1	0	-1	0	1	0	-1	0
CM2	1	0	-1	0	-1	0	1	0	1	0	1	0	1	0	1	0
CM2	1	0	-1	0	-1	0	1	0	1	0	1	0	1	0	1	0
CM1	1	0	1	0	-1	0	-1	0	1	0	-1	0	1	0	-1	0

CORRELATION FUNCTION

N	-15	-14	-13	-12	-11	-10	-9	-8	-7	-6	-5	-4	-3	-2	-1	-0	1	2	3	4	5	6	7	8	9	10	11	12	13	14	15
Z	0	-0	0	8	0	0	0	0	0	-0	0	-8	0	-0	0	0	0	0	0	-8	0	0	0	0	0	-0	0	8	0	0	0

INPUT WAVEFORMS

CS1	1	0	1	0	1	0	1	0	1	0	1	0	-1	0	1	0
CS1	1	0	1	0	1	0	1	0	1	0	1	0	-1	0	1	0
CS2	1	0	-1	0	1	0	-1	0	1	0	-1	0	-1	0	-1	0
CS2	1	0	-1	0	1	0	-1	0	1	0	-1	0	-1	0	-1	0
CS1	1	0	1	0	1	0	1	0	1	0	1	0	-1	0	1	0
CS1	1	0	1	0	1	0	1	0	1	0	1	0	-1	0	1	0
CS2	1	0	-1	0	1	0	-1	0	1	0	-1	0	-1	0	-1	0
CS2	1	0	-1	0	1	0	-1	0	1	0	-1	0	-1	0	-1	0

CORRELATION FUNCTION

N	-15	-14	-13	-12	-11	-10	-9	-8	-7	-6	-5	-4	-3	-2	-1	-0	1	2	3	4	5	6	7	8	9	10	11	12	13	14	15
Z	0	0	0	-0	0	0	0	8	0	0	0	16	0	-0	0	32	0	-0	0	16	0	0	0	8	0	0	0	-0	0	0	0

INPUT WAVEFORMS

CS1	1	0	1	0	1	0	1	0	1	0	1	0	-1	0	1	0
CS2	1	0	-1	0	1	0	-1	0	1	0	-1	0	-1	0	-1	0
CS2	1	0	-1	0	1	0	-1	0	1	0	-1	0	-1	0	-1	0
CS1	1	0	1	0	1	0	1	0	1	0	1	0	-1	0	1	0
CS1	1	0	1	0	1	0	1	0	1	0	1	0	-1	0	1	0
CS2	1	0	-1	0	1	0	-1	0	1	0	-1	0	-1	0	-1	0
CS2	1	0	-1	0	1	0	-1	0	1	0	-1	0	-1	0	-1	0
CS1	1	0	1	0	1	0	1	0	1	0	1	0	-1	0	1	0

CORRELATION FUNCTION

N	-15	-14	-13	-12	-11	-10	-9	-8	-7	-6	-5	-4	-3	-2	-1	-0	1	2	3	4	5	6	7	8	9	10	11	12	13	14	15
Z	0	0	0	-8	0	0	0	-8	0	0	0	-8	0	-0	0	0	0	0	0	-8	0	-0	0	-8	0	-0	0	-8	0	-0	0

INPUT WAVEFORMS

CM1	1	0	1	0	-1	0	-1	0	1	0	-1	0	1	0	-1	0
CS1	1	0	1	0	1	0	1	0	1	0	1	0	-1	0	1	0
CM2	1	0	-1	0	-1	0	1	0	1	0	1	0	1	0	1	0
CS2	1	0	-1	0	1	0	-1	0	1	0	-1	0	-1	0	-1	0
CM1	1	0	1	0	-1	0	-1	0	1	0	-1	0	1	0	-1	0
CS1	1	0	1	0	1	0	1	0	1	0	1	0	-1	0	1	0
CM2	1	0	-1	0	-1	0	1	0	1	0	1	0	1	0	1	0
CS2	1	0	-1	0	1	0	-1	0	1	0	-1	0	-1	0	-1	0

CORRELATION FUNCTION

N	-15	-14	-13	-12	-11	-10	-9	-8	-7	-6	-5	-4	-3	-2	-1	-0	1	2	3	4	5	6	7	8	9	10	11	12	13	14	15
Z	0	-0	0	0	0	-0	0	0	0	-0	0	-8	0	0	0	-8	0	0	0	-8	0	0	0	8	0	-0	0	-0	0	0	0

INPUT WAVEFORMS

CM1	1	0	1	0	-1	0	-1	0	1	0	-1	0	1	0	-1	0
CS2	1	0	-1	0	1	0	-1	0	1	0	-1	0	-1	0	-1	0
CM2	1	0	-1	0	-1	0	1	0	1	0	1	0	1	0	1	0
CS1	1	0	1	0	1	0	1	0	1	0	1	0	-1	0	1	0
CM1	1	0	1	0	-1	0	-1	0	1	0	-1	0	1	0	-1	0
CS2	1	0	-1	0	1	0	-1	0	1	0	-1	0	-1	0	-1	0
CM2	1	0	-1	0	-1	0	1	0	1	0	1	0	1	0	1	0
CS1	1	0	1	0	1	0	1	0	1	0	1	0	-1	0	1	0

CORRELATION FUNCTION

N	-15	-14	-13	-12	-11	-10	-9	-8	-7	-6	-5	-4	-3	-2	-1	-0	1	2	3	4	5	6	7	8	9	10	11	12	13	14	15
Z	0	-0	0	8	0	-0	0	16	0	-0	0	16	0	0	0	8	0	-0	0	-0	0	-0	0	8	0	0	0	-8	0	-0	0

INPUT WAVEFORMS

DM1	1	1	1	1	-1	1	-1	-1	1	1	-1	1	1	-1	-1	1
DM1	1	1	1	1	-1	1	-1	-1	1	1	-1	1	1	-1	-1	1
DM2	1	1	-1	1	-1	1	1	-1	1	-1	1	-1	1	1	1	-1
DM2	1	1	-1	1	-1	1	1	-1	1	-1	1	-1	1	1	1	-1
DM3	1	-1	1	-1	-1	-1	-1	1	1	-1	-1	-1	1	1	-1	-1
DM3	1	-1	1	-1	-1	-1	-1	1	1	-1	-1	-1	1	1	-1	-1
DM4	1	-1	-1	-1	-1	-1	1	1	1	1	1	1	1	-1	1	1
DM4	1	-1	-1	-1	-1	-1	1	1	1	1	1	1	1	-1	1	1

CORRELATION FUNCTION

N	-15	-14	-13	-12	-11	-10	-9	-8	-7	-6	-5	-4	-3	-2	-1	-0	1	2	3	4	5	6	7	8	9	10	11	12	13	14	15
Z	-0	0	0	0	0	0	-0	-0	-0	-0	-0	-0	-0	0	-0	64	-0	0	-0	-0	-0	-0	-0	-0	-0	0	0	0	0	0	-0

INPUT WAVEFORMS

DM1	1	1	1	1	-1	1	-1	-1	1	1	-1	1	1	-1	-1	1
DM2	1	1	-1	1	-1	1	1	-1	1	-1	1	-1	1	1	1	-1
DM2	1	1	-1	1	-1	1	1	-1	1	-1	1	-1	1	1	1	-1
DM3	1	-1	1	-1	-1	-1	-1	1	1	-1	-1	-1	1	1	-1	-1
DM3	1	-1	1	-1	-1	-1	-1	1	1	-1	-1	-1	1	1	-1	-1
DM4	1	-1	-1	-1	-1	-1	1	1	1	1	1	1	1	-1	1	1
DM4	1	-1	-1	-1	-1	-1	1	1	1	1	1	1	1	-1	1	1
DM1	1	1	1	1	-1	1	-1	-1	1	1	-1	1	1	-1	-1	1

CORRELATION FUNCTION

N	-15	-14	-13	-12	-11	-10	-9	-8	-7	-6	-5	-4	-3	-2	-1	-0	1	2	3	4	5	6	7	8	9	10	11	12	13	14	15
Z	-0	4	-0	8	0	4	0	0	-0	12	0	-8	-0	-4	0	-0	-0	4	-0	-8	-0	-12	-0	-0	-0	-4	0	8	0	-4	-0

INPUT WAVEFORMS

DM1	1	1	1	1	-1	1	-1	-1	1	1	-1	1	1	-1	-1	1	
DM3	1	-1	1	-1	-1	-1	-1	1	1	-1	-1	-1	1	1	-1	-1	
DM2	1	1	-1	1	-1	1	1	-1	1	-1	1	-1	1	1	1	-1	
DM4	1	-1	-1	-1	-1	-1	1	1	1	1	1	1	1	-1	1	1	
DM3	1	-1	1	-1	-1	-1	-1	1	1	-1	-1	-1	1	1	-1	-1	
DM1	1	1	1	1	-1	1	-1	-1	1	1	-1	1	1	-1	-1	1	
DM4	1	-1	-1	-1	-1	-1	1	1	1	1	1	1	1	-1	1	1	
DM2	1	1	-1	1	-1	1	1	-1	1	-1	1	-1	1	1	1	-1	

CORRELATION FUNCTION

N	-15	-14	-13	-12	-11	-10	-9	-8	-7	-6	-5	-4	-3	-2	-1	-0	1	2	3	4	5	6	7	8	9	10	11	12	13	14	15
Z	-0	-0	0	-0	0	-0	-0	0	-0	0	-0	0	-0	-0	-0	0	0	-0	0	0	0	0	0	0	0	-0	-0	-0	-0	-0	0

INPUT WAVEFORMS

DM1	1	1	1	1	-1	1	-1	-1	1	1	-1	1	1	-1	-1	1	
DM4	1	-1	-1	-1	-1	-1	1	1	1	1	1	1	1	-1	1	1	
DM2	1	1	-1	1	-1	1	1	-1	1	-1	1	-1	1	1	1	-1	
DM1	1	1	1	1	-1	1	-1	-1	1	1	-1	1	1	-1	-1	1	
DM3	1	-1	1	-1	-1	-1	-1	1	1	-1	-1	-1	1	1	-1	-1	
DM2	1	1	-1	1	-1	1	1	-1	1	-1	1	-1	1	1	1	-1	
DM4	1	-1	-1	-1	-1	-1	1	1	1	1	1	1	1	-1	1	1	
DM3	1	-1	1	-1	-1	-1	-1	1	1	-1	-1	-1	1	1	-1	-1	

CORRELATION FUNCTION

N	-15	-14	-13	-12	-11	-10	-9	-8	-7	-6	-5	-4	-3	-2	-1	-0	1	2	3	4	5	6	7	8	9	10	11	12	13	14	15
Z	-0	-4	-0	8	0	-4	0	-0	-0	-12	0	-8	-0	4	0	0	0	-4	0	-8	0	12	0	0	0	4	-0	8	-0	4	0

INPUT WAVEFORMS

DS1	1	1	1	-1	1	1	1	1	1	-1	-1	-1	-1	-1	1	1	
DS1	1	1	1	-1	1	1	1	1	1	-1	-1	-1	-1	-1	1	1	
DS2	1	1	-1	-1	1	1	-1	1	1	1	1	1	-1	1	-1	-1	
DS2	1	1	-1	-1	1	1	-1	1	1	1	1	1	-1	1	-1	-1	
DS3	1	-1	1	1	1	-1	1	-1	1	1	-1	1	-1	1	1	-1	
DS3	1	-1	1	1	1	-1	1	-1	1	1	-1	1	-1	1	1	-1	
DS4	1	-1	-1	1	1	-1	-1	-1	1	-1	1	-1	-1	-1	-1	1	
DS4	1	-1	-1	1	1	-1	-1	-1	1	-1	1	-1	-1	-1	-1	1	

CORRELATION FUNCTION

N	-15	-14	-13	-12	-11	-10	-9	-8	-7	-6	-5	-4	-3	-2	-1	-0	1	2	3	4	5	6	7	8	9	10	11	12	13	14	15
Z	-0	0	0	-0	-0	0	0	0	-0	0	-0	0	0	0	0	64	0	0	0	0	-0	0	-0	0	0	0	-0	-0	0	0	-0

INPUT WAVEFORMS

DS1	1	1	1	-1	1	1	1	1	1	-1	-1	-1	-1	-1	1	1	
DS2	1	1	-1	-1	1	1	-1	1	1	1	1	1	-1	1	-1	-1	
DS2	1	1	-1	-1	1	1	-1	1	1	1	1	1	-1	1	-1	-1	
DS3	1	-1	1	1	1	-1	1	-1	1	1	-1	1	-1	1	1	-1	
DS3	1	-1	1	1	1	-1	1	-1	1	1	-1	1	-1	1	1	-1	
DS4	1	-1	-1	1	1	-1	-1	-1	1	-1	1	-1	-1	-1	-1	1	
DS4	1	-1	-1	1	1	-1	-1	-1	1	-1	1	-1	-1	-1	-1	1	
DS1	1	1	1	-1	1	1	1	1	1	-1	-1	-1	-1	-1	1	1	

CORRELATION FUNCTION

N	-15	-14	-13	-12	-11	-10	-9	-8	-7	-6	-5	-4	-3	-2	-1	-0	1	2	3	4	5	6	7	8	9	10	11	12	13	14	15
Z	-0	4	-0	-16	-0	4	-0	-0	-0	-4	0	0	0	-4	-0	-0	0	4	0	16	-0	4	-0	0	0	-4	-0	-0	0	-4	-0

INPUT WAVEFORMS

DS1	1	1	1	-1	1	1	1	1	1	-1	-1	-1	-1	-1	1	1
DS3	1	-1	1	1	1	-1	1	-1	1	1	-1	1	-1	1	1	-1
DS2	1	1	-1	-1	1	1	-1	1	1	1	1	1	-1	1	-1	-1
DS4	1	-1	-1	1	1	-1	-1	-1	1	-1	1	-1	-1	-1	-1	1
DS3	1	-1	1	1	1	-1	1	-1	1	1	-1	1	-1	1	1	-1
DS1	1	1	1	-1	1	1	1	1	1	-1	-1	-1	-1	-1	1	1
DS4	1	-1	-1	1	1	-1	-1	-1	1	-1	1	-1	-1	-1	-1	1
DS2	1	1	-1	-1	1	1	-1	1	1	1	1	1	-1	1	-1	-1

CORRELATION FUNCTION

N	-15	-14	-13	-12	-11	-10	-9	-8	-7	-6	-5	-4	-3	-2	-1	-0	1	2	3	4	5	6	7	8	9	10	11	12	13	14	15
Z	-0	-0	0	0	-0	-0	0	-0	-0	-0	-0	-0	0	-0	0	0	-0	-0	-0	-0	0	-0	0	-0	-0	-0	0	0	-0	-0	0

INPUT WAVEFORMS

DS1	1	1	1	-1	1	1	1	1	1	-1	-1	-1	-1	-1	1	1
DS4	1	-1	-1	1	1	-1	-1	-1	1	-1	1	-1	-1	-1	-1	1
DS2	1	1	-1	-1	1	1	-1	1	1	1	1	1	-1	1	-1	-1
DS1	1	1	1	-1	1	1	1	1	1	-1	-1	-1	-1	-1	1	1
DS3	1	-1	1	1	1	-1	1	-1	1	1	-1	1	-1	1	1	-1
DS2	1	1	-1	-1	1	1	-1	1	1	1	1	1	-1	1	-1	-1
DS4	1	-1	-1	1	1	-1	-1	-1	1	-1	1	-1	-1	-1	-1	1
DS3	1	-1	1	1	1	-1	1	-1	1	1	-1	1	-1	1	1	-1

CORRELATION FUNCTION

N	-15	-14	-13	-12	-11	-10	-9	-8	-7	-6	-5	-4	-3	-2	-1	-0	1	2	3	4	5	6	7	8	9	10	11	12	13	14	15
Z	-0	-4	-0	-0	-0	-4	-0	0	-0	4	0	16	0	4	-0	0	-0	-4	-0	-0	0	-4	0	-0	-0	4	0	-16	-0	4	0

INPUT WAVEFORMS

DM1	1	1	1	1	-1	1	-1	-1	1	1	-1	1	1	-1	-1	1
DS1	1	1	1	-1	1	1	1	1	1	-1	-1	-1	-1	-1	1	1
DM2	1	1	-1	1	-1	1	1	-1	1	-1	1	-1	1	1	1	-1
DS2	1	1	-1	-1	1	1	-1	1	1	1	1	1	-1	1	-1	-1
DM3	1	-1	1	-1	-1	-1	-1	1	1	-1	-1	-1	1	1	-1	-1
DS3	1	-1	1	1	1	-1	1	-1	1	1	-1	1	-1	1	1	-1
DM4	1	-1	-1	-1	-1	-1	1	1	1	1	1	1	-1	1	1	1
DS4	1	-1	-1	1	1	-1	-1	-1	1	-1	1	-1	-1	-1	-1	1

CORRELATION FUNCTION

N	-15	-14	-13	-12	-11	-10	-9	-8	-7	-6	-5	-4	-3	-2	-1	-0	1	2	3	4	5	6	7	8	9	10	11	12	13	14	15
Z	-0	0	0	-0	-0	0	0	0	-0	-8	-0	8	0	-8	0	-0	-0	-8	-0	8	-0	8	-0	-0	-0	0	0	0	0	0	-0

INPUT WAVEFORMS

DM1	1	1	1	1	-1	1	-1	-1	1	1	-1	1	1	-1	-1	1
DS2	1	1	-1	-1	1	1	-1	1	1	1	1	1	-1	1	-1	-1
DM2	1	1	-1	1	-1	1	1	-1	1	-1	1	-1	1	1	1	-1
DS3	1	-1	1	1	1	-1	1	-1	1	1	-1	1	-1	1	1	-1
DM3	1	-1	1	-1	-1	-1	-1	1	1	-1	-1	-1	1	1	-1	-1
DS4	1	-1	-1	1	1	-1	-1	-1	1	-1	1	-1	-1	-1	-1	1
DM4	1	-1	-1	-1	-1	-1	1	1	1	1	1	1	-1	1	1	1
DS1	1	1	1	-1	1	1	1	1	1	-1	-1	-1	-1	-1	1	1

CORRELATION FUNCTION

N	-15	-14	-13	-12	-11	-10	-9	-8	-7	-6	-5	-4	-3	-2	-1	-0	1	2	3	4	5	6	7	8	9	10	11	12	13	14	15
Z	-0	4	-0	0	-0	12	-0	16	-0	-4	0	16	0	4	-0	-0	-0	-4	-0	-8	-0	4	-0	32	-0	4	0	-8	0	-4	-0

INPUT WAVEFORMS

DM1	1	1	1	1	-1	1	-1	-1	1	1	-1	1	1	-1	-1	1
DS3	1	-1	1	1	1	-1	1	-1	1	1	-1	1	-1	1	1	-1
DM2	1	1	-1	1	-1	1	1	-1	1	-1	1	-1	1	1	1	-1
DS4	1	-1	-1	1	1	-1	-1	-1	1	-1	1	-1	-1	-1	-1	1
DM3	1	-1	1	-1	-1	-1	-1	1	1	-1	-1	-1	1	1	-1	-1
DS1	1	1	1	-1	1	1	1	1	1	-1	-1	-1	-1	-1	1	1
DM4	1	-1	-1	-1	-1	-1	1	1	1	1	1	1	1	-1	1	1
DS2	1	1	-1	-1	1	1	-1	1	1	1	1	1	-1	1	-1	-1

CORRELATION FUNCTION

N	-15	-14	-13	-12	-11	-10	-9	-8	-7	-6	-5	-4	-3	-2	-1	-0	1	2	3	4	5	6	7	8	9	10	11	12	13	14	15
Z	-0	-0	0	0	-0	-0	0	-0	-0	8	-0	-8	0	8	0	0	0	8	0	-8	0	-8	0	0	0	-0	-0	-0	-0	-0	0

INPUT WAVEFORMS

DM1	1	1	1	1	-1	1	-1	-1	1	1	-1	1	1	-1	-1	1
DS4	1	-1	-1	1	1	-1	-1	-1	1	-1	1	-1	-1	-1	-1	1
DM2	1	1	-1	1	-1	1	1	-1	1	-1	1	-1	1	1	1	-1
DS1	1	1	1	-1	1	1	1	1	1	-1	-1	-1	-1	-1	1	1
DM3	1	-1	1	-1	-1	-1	-1	1	1	-1	-1	-1	1	1	-1	-1
DS2	1	1	-1	-1	1	1	-1	1	1	1	1	1	-1	1	-1	-1
DM4	1	-1	-1	-1	-1	-1	1	1	1	1	1	1	1	-1	1	1
DS3	1	-1	1	1	1	-1	1	-1	1	1	-1	1	-1	1	1	-1

CORRELATION FUNCTION

N	-15	-14	-13	-12	-11	-10	-9	-8	-7	-6	-5	-4	-3	-2	-1	-0	1	2	3	4	5	6	7	8	9	10	11	12	13	14	15
Z	-0	-4	-0	16	-0	-12	-0	16	-0	4	0	-0	0	-4	-0	0	0	4	0	-8	0	-4	0	0	0	-4	-0	-8	-0	4	0

INPUT WAVEFORMS

CM1	1	0	1	0	-1	0	-1	0	1	0	-1	0	1	0	-1	0
DM1	1	1	1	1	-1	1	-1	-1	1	1	-1	1	1	-1	-1	1
CM2	1	0	-1	0	-1	0	1	0	1	0	1	0	1	0	1	0
DM2	1	1	-1	1	-1	1	1	-1	1	-1	1	-1	1	1	1	-1
CM1	1	0	1	0	-1	0	-1	0	1	0	-1	0	1	0	-1	0
DM3	1	-1	1	-1	-1	-1	-1	1	1	-1	-1	-1	1	1	-1	-1
CM2	1	0	-1	0	-1	0	1	0	1	0	1	0	1	0	1	0
DM4	1	-1	-1	-1	-1	-1	1	1	1	1	1	1	1	-1	1	1

CORRELATION FUNCTION

N	-15	-14	-13	-12	-11	-10	-9	-8	-7	-6	-5	-4	-3	-2	-1	-0	1	2	3	4	5	6	7	8	9	10	11	12	13	14	15
Z	0	-0	0	0	0	0	0	-0	-0	-0	-0	-0	-0	-0	0	32	-0	-0	-0	-0	-0	-0	-0	-0	-0	0	0	0	0	-0	-0

INPUT WAVEFORMS

CM1	1	0	1	0	-1	0	-1	0	1	0	-1	0	1	0	-1	0
DM2	1	1	-1	1	-1	1	1	-1	1	-1	1	-1	1	1	1	-1
CM2	1	0	-1	0	-1	0	1	0	1	0	1	0	1	0	1	0
DM3	1	-1	1	-1	-1	-1	-1	1	1	-1	-1	-1	1	1	-1	-1
CM1	1	0	1	0	-1	0	-1	0	1	0	-1	0	1	0	-1	0
DM4	1	-1	-1	-1	-1	-1	1	1	1	1	1	1	1	-1	1	1
CM2	1	0	-1	0	-1	0	1	0	1	0	1	0	1	0	1	0
DM1	1	1	1	1	-1	1	-1	-1	1	1	-1	1	1	-1	-1	1

CORRELATION FUNCTION

N	-15	-14	-13	-12	-11	-10	-9	-8	-7	-6	-5	-4	-3	-2	-1	-0	1	2	3	4	5	6	7	8	9	10	11	12	13	14	15
Z	0	-0	-0	8	-0	0	-0	0	0	-0	-0	-8	-0	-0	0	0	-0	0	-0	-8	-0	0	-0	0	-0	-0	0	8	0	0	-0

INPUT WAVEFORMS

CM1	1	0	1	0	-1	0	-1	0	1	0	-1	0	1	0	-1	0
DM3	1	-1	1	-1	-1	-1	-1	1	1	-1	-1	-1	1	1	-1	-1
CM2	1	0	-1	0	-1	0	1	0	1	0	1	0	1	0	1	0
DM4	1	-1	-1	-1	-1	-1	1	1	1	1	1	1	1	-1	1	1
CM1	1	0	1	0	-1	0	-1	0	1	0	-1	0	1	0	-1	0
DM1	1	1	1	1	-1	1	-1	-1	1	1	-1	1	1	-1	-1	1
CM2	1	0	-1	0	-1	0	1	0	1	0	1	0	1	0	1	0
DM2	1	1	-1	1	-1	1	1	-1	1	-1	1	-1	1	1	1	-1

CORRELATION FUNCTION

N	-15	-14	-13	-12	-11	-10	-9	-8	-7	-6	-5	-4	-3	-2	-1	-0	1	2	3	4	5	6	7	8	9	10	11	12	13	14	15
Z	0	-0	-0	0	-0	0	-0	-0	0	-0	0	-0	0	-0	-0	32	0	-0	0	-0	0	-0	0	-0	0	0	-0	0	-0	-0	0

INPUT WAVEFORMS

CM1	1	0	1	0	-1	0	-1	0	1	0	-1	0	1	0	-1	0
DM4	1	-1	-1	-1	-1	-1	1	1	1	1	1	1	1	-1	1	1
CM2	1	0	-1	0	-1	0	1	0	1	0	1	0	1	0	1	0
DM1	1	1	1	1	-1	1	-1	-1	1	1	-1	1	1	-1	-1	1
CM1	1	0	1	0	-1	0	-1	0	1	0	-1	0	1	0	-1	0
DM2	1	1	-1	1	-1	1	1	-1	1	-1	1	-1	1	1	1	-1
CM2	1	0	-1	0	-1	0	1	0	1	0	1	0	1	0	1	0
DM3	1	-1	1	-1	-1	-1	-1	1	1	-1	-1	-1	1	1	-1	-1

CORRELATION FUNCTION

N	-15	-14	-13	-12	-11	-10	-9	-8	-7	-6	-5	-4	-3	-2	-1	-0	1	2	3	4	5	6	7	8	9	10	11	12	13	14	15
Z	0	-0	0	8	0	0	0	0	-0	-0	0	-8	0	-0	-0	0	0	0	0	-8	0	0	0	0	0	-0	-0	8	-0	0	0

INPUT WAVEFORMS

CM1	1	0	1	0	-1	0	-1	0	1	0	-1	0	1	0	-1	0
DS1	1	1	1	-1	1	1	1	1	1	-1	-1	-1	-1	-1	1	1
CM2	1	0	-1	0	-1	0	1	0	1	0	1	0	1	0	1	0
DS2	1	1	-1	-1	1	1	-1	1	1	1	1	1	-1	1	-1	-1
CM1	1	0	1	0	-1	0	-1	0	1	0	-1	0	1	0	-1	0
DS3	1	-1	1	1	1	-1	1	-1	1	1	-1	1	-1	1	1	-1
CM2	1	0	-1	0	-1	0	1	0	1	0	1	0	1	0	1	0
DS4	1	-1	-1	1	1	-1	-1	-1	1	-1	1	-1	-1	-1	-1	1

CORRELATION FUNCTION

N	-15	-14	-13	-12	-11	-10	-9	-8	-7	-6	-5	-4	-3	-2	-1	-0	1	2	3	4	5	6	7	8	9	10	11	12	13	14	15
Z	0	-0	0	0	-0	-0	0	0	0	-0	0	-0	0	0	0	0	-0	0	-0	0	-0	0	-0	0	-0	-0	0	-0	0	0	-0

INPUT WAVEFORMS

CM1	1	0	1	0	-1	0	-1	0	1	0	-1	0	1	0	-1	0
DS2	1	1	-1	-1	1	1	-1	1	1	1	1	1	-1	1	-1	-1
CM2	1	0	-1	0	-1	0	1	0	1	0	1	0	1	0	1	0
DS3	1	-1	1	1	1	-1	1	-1	1	1	-1	1	-1	1	1	-1
CM1	1	0	1	0	-1	0	-1	0	1	0	-1	0	1	0	-1	0
DS4	1	-1	-1	1	1	-1	-1	-1	1	-1	1	-1	-1	-1	-1	1
CM2	1	0	-1	0	-1	0	1	0	1	0	1	0	1	0	1	0
DS1	1	1	1	-1	1	1	1	1	1	-1	-1	-1	-1	-1	1	1

CORRELATION FUNCTION

N	-15	-14	-13	-12	-11	-10	-9	-8	-7	-6	-5	-4	-3	-2	-1	-0	1	2	3	4	5	6	7	8	9	10	11	12	13	14	15
Z	0	-0	-0	8	0	-0	-0	16	-0	-0	0	8	0	0	0	-0	-0	-0	-0	-8	-0	-0	-0	16	-0	0	0	-8	0	-0	-0

INPUT WAVEFORMS

CM1	1	0	1	0	-1	0	-1	0	1	0	-1	0	1	0	-1	0
DS3	1	-1	1	1	1	-1	1	-1	1	1	-1	1	-1	1	1	-1
CM2	1	0	-1	0	-1	0	1	0	1	0	1	0	1	0	1	0
DS4	1	-1	-1	1	1	-1	-1	-1	1	-1	1	-1	-1	-1	-1	1
CM1	1	0	1	0	-1	0	-1	0	1	0	-1	0	1	0	-1	0
DS1	1	1	1	-1	1	1	1	1	1	-1	-1	-1	-1	-1	1	1
CM2	1	0	-1	0	-1	0	1	0	1	0	1	0	1	0	1	0
DS2	1	1	-1	-1	1	1	-1	1	1	1	1	1	-1	1	-1	-1

CORRELATION FUNCTION

N	-15	-14	-13	-12	-11	-10	-9	-8	-7	-6	-5	-4	-3	-2	-1	-0	1	2	3	4	5	6	7	8	9	10	11	12	13	14	15
Z	0	-0	-0	0	0	-0	-0	0	-0	-0	-0	-0	-0	0	-0	0	0	0	0	0	0	0	0	0	0	-0	-0	-0	-0	0	0

INPUT WAVEFORMS

CM1	1	0	1	0	-1	0	-1	0	1	0	-1	0	1	0	-1	0
DS4	1	-1	-1	1	1	-1	-1	-1	1	-1	1	-1	-1	-1	-1	1
CM2	1	0	-1	0	-1	0	1	0	1	0	1	0	1	0	1	0
DS1	1	1	1	-1	1	1	1	1	1	-1	-1	-1	-1	-1	1	1
CM1	1	0	1	0	-1	0	-1	0	1	0	-1	0	1	0	-1	0
DS2	1	1	-1	-1	1	1	-1	1	1	1	1	1	-1	1	-1	-1
CM2	1	0	-1	0	-1	0	1	0	1	0	1	0	1	0	1	0
DS3	1	-1	1	1	1	-1	1	-1	1	1	-1	1	-1	1	1	-1

CORRELATION FUNCTION

N	-15	-14	-13	-12	-11	-10	-9	-8	-7	-6	-5	-4	-3	-2	-1	-0	1	2	3	4	5	6	7	8	9	10	11	12	13	14	15
Z	0	-0	0	8	-0	-0	0	16	0	-0	-0	8	-0	0	-0	-0	0	-0	0	-8	0	-0	0	16	0	0	-0	-8	-0	-0	0

INPUT WAVEFORMS

CS1	1	0	1	0	1	0	1	0	1	0	1	0	-1	0	1	0
DM1	1	1	1	1	-1	1	-1	-1	1	1	-1	1	1	-1	-1	1
CS2	1	0	-1	0	1	0	-1	0	1	0	-1	0	-1	0	-1	0
DM2	1	1	-1	1	-1	1	1	-1	1	-1	1	-1	1	1	1	-1
CS1	1	0	1	0	1	0	1	0	1	0	1	0	-1	0	1	0
DM3	1	-1	1	-1	-1	-1	-1	1	1	-1	-1	-1	1	1	-1	-1
CS2	1	0	-1	0	1	0	-1	0	1	0	-1	0	-1	0	-1	0
DM4	1	-1	-1	-1	-1	-1	1	1	1	1	1	1	-1	1	1	

CORRELATION FUNCTION

N	-15	-14	-13	-12	-11	-10	-9	-8	-7	-6	-5	-4	-3	-2	-1	-0	1	2	3	4	5	6	7	8	9	10	11	12	13	14	15
Z	0	0	-0	-0	-0	-0	-0	8	0	0	0	-8	0	0	-0	-8	0	0	0	-8	0	-0	-0	0	0	-0	-0	0	0	-0	-0

INPUT WAVEFORMS

CS1	1	0	1	0	1	0	1	0	1	0	1	0	-1	0	1	0
DM2	1	1	-1	1	-1	1	1	-1	1	-1	1	-1	1	1	1	-1
CS2	1	0	-1	0	1	0	-1	0	1	0	-1	0	-1	0	-1	0
DM3	1	-1	1	-1	-1	-1	-1	1	1	-1	-1	-1	1	1	-1	-1
CS1	1	0	1	0	1	0	1	0	1	0	1	0	-1	0	1	0
DM4	1	-1	-1	-1	-1	-1	1	1	1	1	1	1	-1	1	1	
CS2	1	0	-1	0	1	0	-1	0	1	0	-1	0	-1	0	-1	0
DM1	1	1	1	1	-1	1	-1	-1	1	1	-1	1	1	-1	-1	1

CORRELATION FUNCTION

N	-15	-14	-13	-12	-11	-10	-9	-8	-7	-6	-5	-4	-3	-2	-1	-0	1	2	3	4	5	6	7	8	9	10	11	12	13	14	15
Z	0	0	0	-8	0	-0	0	8	-0	0	0	-0	0	0	-0	8	0	-0	0	16	0	0	-0	16	0	0	-0	8	0	0	-0

INPUT WAVEFORMS

CS1	1	0	1	0	1	0	1	0	1	0	1	0	-1	0	1	0
DM3	1	-1	1	-1	-1	-1	-1	1	1	-1	-1	-1	1	1	-1	-1
CS2	1	0	-1	0	1	0	-1	0	1	0	-1	0	-1	0	-1	0
DM4	1	-1	-1	-1	-1	-1	1	1	1	1	1	1	1	-1	1	1
CS1	1	0	1	0	1	0	1	0	1	0	1	0	-1	0	1	0
DM1	1	1	1	1	-1	1	-1	-1	1	1	-1	1	1	-1	-1	1
CS2	1	0	-1	0	1	0	-1	0	1	0	-1	0	-1	0	-1	0
DM2	1	1	-1	1	-1	1	1	-1	1	-1	1	-1	1	1	1	-1

CORRELATION FUNCTION

N	-15	-14	-13	-12	-11	-10	-9	-8	-7	-6	-5	-4	-3	-2	-1	-0	1	2	3	4	5	6	7	8	9	10	11	12	13	14	15
Z	0	0	0	-0	0	-0	0	8	-0	0	-0	-8	-0	0	0	-8	-0	0	-0	-8	-0	-0	0	0	-0	-0	0	0	-0	-0	0

INPUT WAVEFORMS

CS1	1	0	1	0	1	0	1	0	1	0	1	0	-1	0	1	0
DM4	1	-1	-1	-1	-1	-1	1	1	1	1	1	1	1	-1	1	1
CS2	1	0	-1	0	1	0	-1	0	1	0	-1	0	-1	0	-1	0
DM1	1	1	1	1	-1	1	-1	-1	1	1	-1	1	1	-1	-1	1
CS1	1	0	1	0	1	0	1	0	1	0	1	0	-1	0	1	0
DM2	1	1	-1	1	-1	1	1	-1	1	-1	1	-1	1	1	1	-1
CS2	1	0	-1	0	1	0	-1	0	1	0	-1	0	-1	0	-1	0
DM3	1	-1	1	-1	-1	-1	-1	1	1	-1	-1	-1	1	1	-1	-1

CORRELATION FUNCTION

N	-15	-14	-13	-12	-11	-10	-9	-8	-7	-6	-5	-4	-3	-2	-1	-0	1	2	3	4	5	6	7	8	9	10	11	12	13	14	15
Z	0	0	-0	-8	-0	-0	-0	8	0	0	-0	-0	-0	0	0	8	-0	-0	-0	16	-0	0	0	16	-0	0	0	8	-0	0	0

INPUT WAVEFORMS

CS1	1	0	1	0	1	0	1	0	1	0	1	0	-1	0	1	0
DS1	1	1	1	-1	1	1	1	1	1	-1	-1	-1	-1	-1	1	1
CS2	1	0	-1	0	1	0	-1	0	1	0	-1	0	-1	0	-1	0
DS2	1	1	-1	-1	1	1	-1	1	1	1	1	1	-1	1	-1	-1
CS1	1	0	1	0	1	0	1	0	1	0	1	0	-1	0	1	0
DS3	1	-1	1	1	1	-1	1	-1	1	1	-1	1	-1	1	1	-1
CS2	1	0	-1	0	1	0	-1	0	1	0	-1	0	-1	0	-1	0
DS4	1	-1	-1	1	1	-1	-1	-1	1	-1	1	-1	-1	-1	-1	1

CORRELATION FUNCTION

N	-15	-14	-13	-12	-11	-10	-9	-8	-7	-6	-5	-4	-3	-2	-1	-0	1	2	3	4	5	6	7	8	9	10	11	12	13	14	15
Z	0	0	-0	-0	0	0	-0	8	-0	0	-0	8	-0	-0	-0	24	0	-0	0	8	0	0	-0	-0	0	0	-0	-0	0	0	-0

INPUT WAVEFORMS

CS1	1	0	1	0	1	0	1	0	1	0	1	0	-1	0	1	0
DS2	1	1	-1	-1	1	1	-1	1	1	1	1	1	-1	1	-1	-1
CS2	1	0	-1	0	1	0	-1	0	1	0	-1	0	-1	0	-1	0
DS3	1	-1	1	1	1	-1	1	-1	1	1	-1	1	-1	1	1	-1
CS1	1	0	1	0	1	0	1	0	1	0	1	0	-1	0	1	0
DS4	1	-1	-1	1	1	-1	-1	-1	1	-1	1	-1	-1	-1	-1	1
CS2	1	0	-1	0	1	0	-1	0	1	0	-1	0	-1	0	-1	0
DS1	1	1	1	-1	1	1	1	1	1	-1	-1	-1	-1	-1	1	1

CORRELATION FUNCTION

N	-15	-14	-13	-12	-11	-10	-9	-8	-7	-6	-5	-4	-3	-2	-1	-0	1	2	3	4	5	6	7	8	9	10	11	12	13	14	15
Z	0	0	0	-8	-0	0	0	-8	0	0	-0	-0	-0	-0	-0	8	0	0	0	0	0	-0	-0	0	0	-0	-0	-8	0	-0	-0

INPUT WAVEFORMS

CS1	1	0	1	0	1	0	1	0	1	0	1	0	-1	0	1	0
DS3	1	-1	1	1	1	-1	1	-1	1	1	-1	1	-1	1	1	-1
CS2	1	0	-1	0	1	0	-1	0	1	0	-1	0	-1	0	-1	0
DS4	1	-1	-1	1	1	-1	-1	-1	1	-1	1	-1	-1	-1	-1	1
CS1	1	0	1	0	1	0	1	0	1	0	1	0	-1	0	1	0
DS1	1	1	1	-1	1	1	1	1	1	-1	-1	-1	-1	-1	1	1
CS2	1	0	-1	0	1	0	-1	0	1	0	-1	0	-1	0	-1	0
DS2	1	1	-1	-1	1	1	-1	1	1	1	1	1	-1	1	-1	-1

CORRELATION FUNCTION

N	-15	-14	-13	-12	-11	-10	-9	-8	-7	-6	-5	-4	-3	-2	-1	-0	1	2	3	4	5	6	7	8	9	10	11	12	13	14	15
Z	0	0	0	-0	-0	0	0	8	0	0	0	8	0	-0	0	24	-0	-0	-0	8	-0	0	0	-0	-0	0	0	-0	-0	0	0

INPUT WAVEFORMS

CS1	1	0	1	0	1	0	1	0	1	0	1	0	-1	0	1	0
DS4	1	-1	-1	1	1	-1	-1	-1	1	-1	1	-1	-1	-1	-1	1
CS2	1	0	-1	0	1	0	-1	0	1	0	-1	0	-1	0	-1	0
DS1	1	1	1	-1	1	1	1	1	1	-1	-1	-1	-1	-1	1	1
CS1	1	0	1	0	1	0	1	0	1	0	1	0	-1	0	1	0
DS2	1	1	-1	-1	1	1	-1	1	1	1	1	1	-1	1	-1	-1
CS2	1	0	-1	0	1	0	-1	0	1	0	-1	0	-1	0	-1	0
DS3	1	-1	1	1	1	-1	1	-1	1	1	-1	1	-1	1	1	-1

CORRELATION FUNCTION

N	-15	-14	-13	-12	-11	-10	-9	-8	-7	-6	-5	-4	-3	-2	-1	-0	1	2	3	4	5	6	7	8	9	10	11	12	13	14	15
Z	0	0	-0	-8	0	0	-0	-8	-0	0	0	-0	0	-0	0	8	-0	0	-0	0	-0	-0	0	0	-0	-0	0	-8	-0	-0	0

INPUT WAVEFORMS

**** ALL INPUT DATA HAVE BEEN PROCESSED
AT LOC 15231

similar to the autocorrelation function in that the envelope will appears as a series of polarized triangles having the same form as the single-pulse autocorrelation function. The amplitude and polarization of the triangles can be determined from the pulse coding (see Table 2). This function is representative of the spurious signal expected from a correlation detector which is searching for either the master or the slave signals.

3.3 Power Spectrum

The power spectrum envelope is also readily obtained from the autocorrelation function. (See Fig. 5)

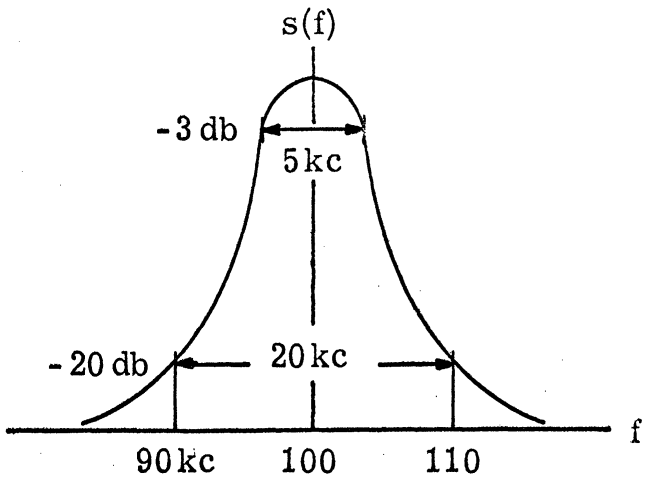

Fig. 5. Signal power spectrum.

Within the envelope are spectral lines at 1-kc spacing and broadened somewhat by the pulse coding. Using this information, the Loran-C receiver, not knowing the phase of the pulse groups within the basic interval and knowing the carrier frequency within only 0.2 cps, must extract the time differences of arrival of the signals within 0.1 μs.

3.4 Anti-jam Margin

The anti-jam margin, defined as AJ = 2WT, in which W is the system bandwidth and T is the integration time, is a good measure of the resistance of the Loran-C/D system to correlated and uncorrelated interference. For Loran-C/D systems, W is the channel bandwidth (20 kc) and T is the basic period (about 100 ms). Accordingly then,

$$AJ = 4000 = 36 \text{ db} .$$

This figure may be interpreted in various ways. First, from the sampling theorem, it represents the number of independent voltage (or current) samples necessary to represent completely the time-domain signal. Second, it represents a rough measure of the potential resistance of a receiver to jamming, say from a cochannel station. (The current Loran-C system does not nearly realize this potential.) Third, it gives an idea of the signal-to-noise improvement possible through correlational techniques; in these cases the improvement is represented by

$$(S/N)_{out} = 2WT(E/N_o)_{in} ,$$

where E/N_o is the input energy-to-noise spectral density ratio. Apparently then, it is possible through optimal coding and detection techniques to achieve a 36-db improvement in the signal-to-noise ratio by coherent integration. Current techniques realize something on the order of 10-20 db.

4. INTERFERENCE MODEL

Signals at 100-kc received over a 2000-4000-km path will be corrupted with the following types of noise: (1) White Gaussian noise (whiganoi) introduced by the receiver input circuitry, (2) atmospheric static noises (sferics), primarily non-Gaussian and impulsive in nature, (3) cochannel cw and pulse signals, and (4) delayed replicas of the Loran-C signal (skywaves).

4.1 Whiganoi

Operating experience has placed the limit on the coverage range for the Loran-C system as the 10 μv/m groundwave contour (A8). With present transmitters and antennas which radiate one megawatt at the sampling point, the 10 μv/m contour occurs at about 4000 km over seawater paths. Receiving antennas have typical effective heights of a tenth of a meter and radiation resistances of about 10^{-6} ohm. Although the available power at the 10 μv/m countour is something like -43 dbm, the small receiving antenna size and radiation resistance lower the antenna efficiency markedly, and, in practice, intercepted powers at -100 dbm are more common.

The sensitivity of any receiver is limited ultimately by whiganoi introduced in the antenna and input circuitry. The available power from this source depends on the bandwidth and circuit temperature,

$$N = kTW,$$

where k is Boltzmann's constant, T is the absolute temperature, and W

is the system bandwidth. The spectral density for typical circuits is then about -174 dbm per cycle of bandwidth. Wiganoi power in a 20 kc bandwidth is -134 dbm. For present receiver noise figures of a few db, then, the signal-to-whiganoi ratio is at least 30 db. Compared to other noise processes, which may be 20 db above 10 μ/m at these frequencies, whiganoi may apparently be neglected.

4.2 Sferics

Atmospheric noise at these frequencies (100 kc) is primarily due to lightning discharges (B1, B2). The discharge spectrum is distinctly off-white, with a broad peak at 3 - 10 kc, tailing off to the microwave range. The time waveform consists of between one and five spikes about 100 μs wide and spaced at about a millisecond. Figure 6 shows one of these spikes, and Fig. 7 shows its spectrum.

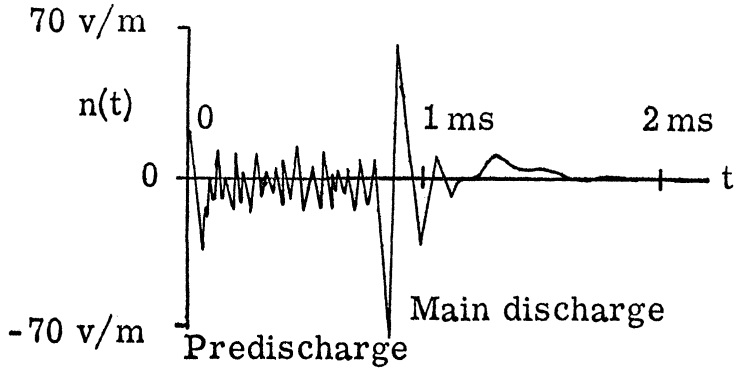

Fig. 6. Sferic time waveform (from B2).

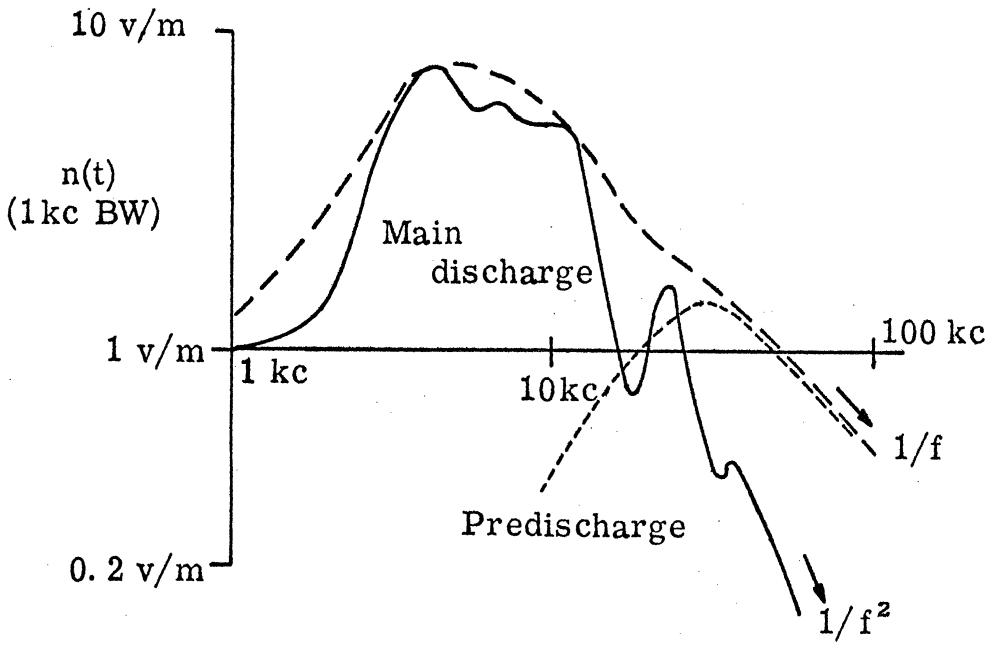

Fig. 7. Sferic power spectrum (from B2).

Apparently this type of signal is similar enough to the Loran-C signal to limit the system performance when the signal-to-sferic ratio is less than -20 db. Questions remain concerning the definition of sferic power due to its impulsive nature. At these frequencies the disturbances generated by a discharge are propagated for a considerable distance, so the receiver noise is the sum of large numbers of these discharges occurring all over the world. The CCIR has established "Noise Grades" in various regions of the world; these apparently are related to the sferic powers. Based on these data, sferic noise powers appear 0-10 db above 10 μv/m during the day and 10-20 db above 10 μv/m during the night in most parts of the world.

4.3 Cochannel Signals

The interference processes discussed above possess rather small autocorrelation functions and, of course, negligible (long term) cross-correlations with the Loran-C/D signals. Judging from the complexity of predetection narrowband filtering equipment of current Loran-C receivers, particular difficulty is experienced with cochannel cw signals. These maintain huge autocorrelation functions but reasonably small cross-correlations with the Loran-C signal if the cw signal is not on a Loran-C spectral line. The problem is evidently not one of correlation but of receiver integrator overloading. Since this is a hardware problem, the cw interference process will be impudently (or imprudently) ignored for the present.

Cochannel Loran-C signals, on the other hand, will be the rule rather than the exception. Interference from cochannel stations includes that from the other stations of the net. Since at a given time the receiver may be hunting for either the master or one of the slaves, the two must be distinguishable. This is done by coding the master pulses differently from the slaves. Once the master pulses have been found, the slaves can then be distinguished by their time sequence relative to the master. The master and slave codings are chosen to have small crosscorrelations, thereby simplifying the acquisition process. In extreme cases, the ratio between the desired signal and the undesired signal powers may approach 80 db when the receiver is parked at 5000 feet over one of the transmitters.

More realistic cases have been computed (A9), and ratios of 30 db are typical on North Atlantic paths near existing stations (see Fig. 8).

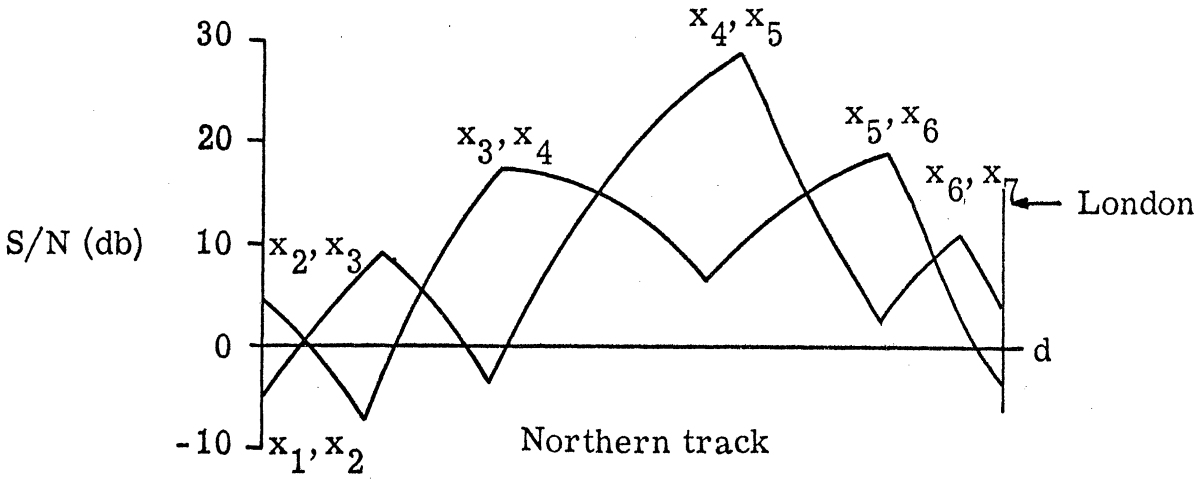

Fig. 8. Differential amplitudes on a North Altantic path (from A9).

Interference from other cochannel nets may be expected in some instances. We will assume here that a cochannel net will have a different basic repetition interval and that it will be sufficiently weak to prevent overloading the integrators during search. (During tracking the integrators are gated.) Then the crosscorrelation becomes small if the integration times much exceed the reciprocal of the smallest difference between the basic intervals. Assuming reasonable ingenuity in siting, and maybe even directional antennas (!), integration times of a second would seem to suffice.

4.4 Skywaves

Multipath skywaves are by far the most perplexing problem in Loran-C operation. In certain regions these may be up to 35 db stronger than the groundwave and may chase the groundwaves at delays of as little as 30 μs (A1, A4). The skywaves may occur as a result of one to five hops and may ricochet around the world for many milliseconds. We will examine this process more closely to gain some insight into the design problems inherent in the receiver.

Consider the over-the-horizon path illustrated in Fig. 9.

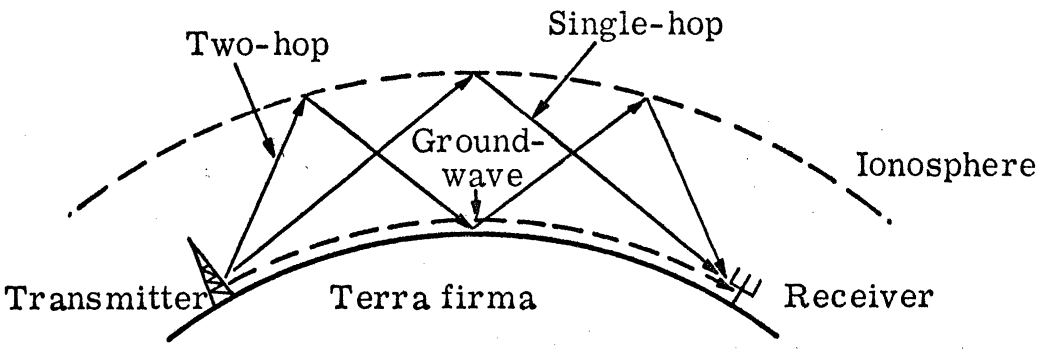

Fig. 9. Multipath skywaves.

This path has an attenuation-distance relation as sketched in Fig. 10. The groundwave intensity is quite close to the inverse-square relationship, except at the limits of the service area. Since the skywaves lose 20-40 db on every bounce, they can be neglected in the inverse-square region. At the further extremities of the service area the delays between multipath signals can be assumed small, at least for one- or two-hop skywaves.

But, in any case, the skywaves will come chasing the groundwaves at spacings of as little as 30 μs, as previously noted.

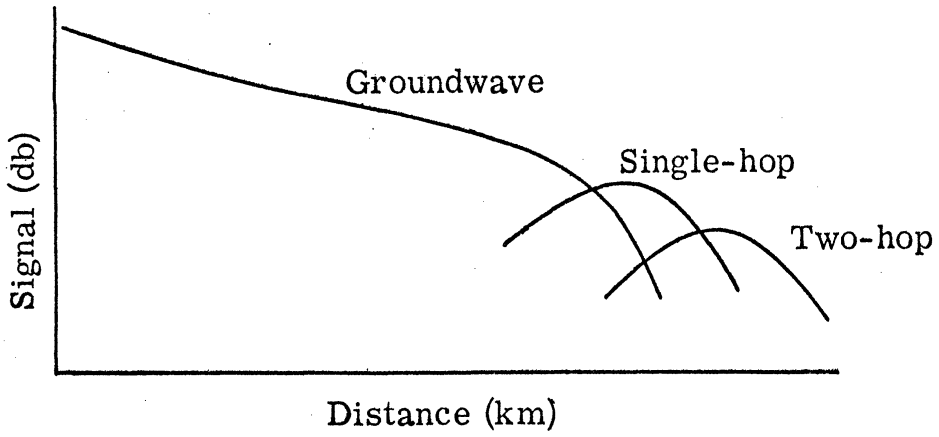

Fig. 10. Skywave intensities.

These combined factors suggest a model for skywave interference consisting of a large first-hop skywave following the groundwave but more-or-less within the groundwave pulse. Thus, each groundwave pulse may be badly distorted by a superimposed, closely following first-hop skywave pulse, but the skywave pulse will not distort succeeding groundwave pulses. The signal intensity of second- and higher-hopped skywave pulses may be assumed of the order of the groundwave, but these skywave pulses may overlap the succeeding pulses of a particular groundwave.

The Loran-C/D phase-coding schemes insure that the autocorrelation of the signal is very small for time displacements of multiples of the interpulse period (1 ms). Thus, the ambiguity in finding a particular

pulse in the multi-pulse group is resolved even in the presence of sky-waves which overlap following groundwave pulses. To achieve this resolution the integration process must extend over the complete basic period.

Resolution of the groundwave and a closely followling high-amplitude skywave cannot be done entirely by linear integration. Assuming the groundwave pulse is free from uncorrelated energy (after any integration), then the detector must identify the third positive-going zero-crossing and this is in an environment of a peak third-cycle to maximum-cycle ratio of 50-60 db in the signal pulse. Obviously nonlinear techniques (clipping, gating, etc.) are in order here.

5. SIGNAL RECOVERY

We apply the word "recovery" to any process intended to yield a time-of-arrival measurement from the received signal. Using the signal model developed in Section 3 and the interference model developed in Section 4, we will attempt to construct appropriate recovery philosophies.

First, we must establish the system parameters and the requisite processing. Since most linear integrators cannot be expected to work well in noise environments 80 db above the signal, a preintegration gate system seems appropriate. The receiver design will then look something like that shown in Fig. 11.

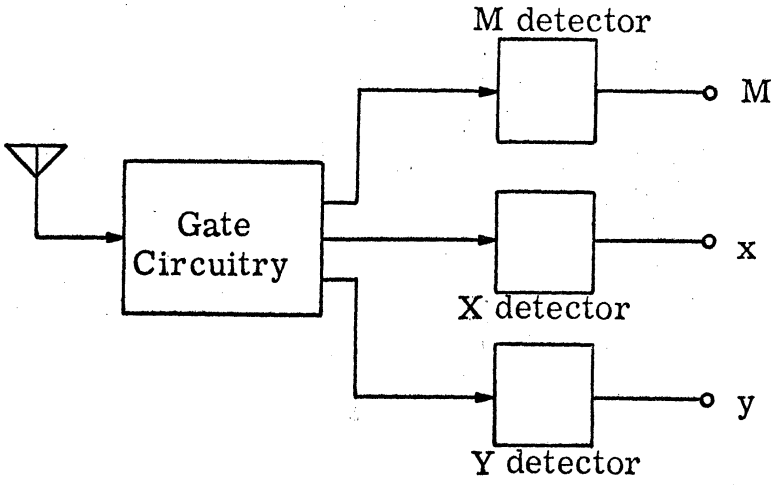

Fig. 11. Predetection gating.

Here the M, X, and Y detectors perform the necessary envelope and phase extractions, and the gate circuitry assigns an interval in time in which to expect the appropriate signal. Actually the X and Y detectors can be combined since the slaves trasmit the same signal and since any ambiguity

is resolved once the M signal is known. The condition in which the detectors are properly gated will be called the tracking condition, and the condition in which the gate circuitry is hunting for the proper time slots, the acquisition condition. In the tracking condition, the detectors can easily servo the gate circuitry to maintain the proper time synchronism, but in the acquisition condition this information is not generally available from the detectors. We suspect that the acquisition stage will be rather difficult.

5.1 Carrier Phase

Let us apply the signal from a Loran-C transmitter to a receiver designed to announce the time of arrival of a pulse group. More specifically, let us consider each pulse of a 100-kc carrier (diagrammed in Fig. 12).

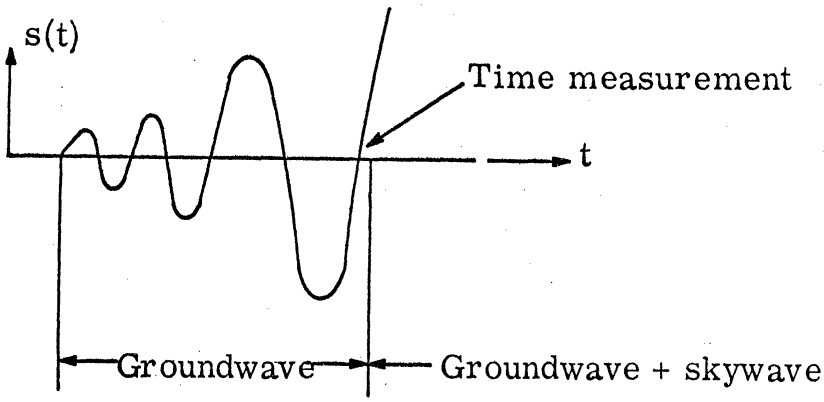

Fig. 12. Detector signal.

Apparently the minimum delay between the time of arrival of the ground wave and that of the skywave is greater than 30 μs, i.e., 3 cycles of a 100-kc carrier. It is highly desirable to confine all time measurements to this initial interval on each pulse in the group.

An accuracy of 0.1-μs time measurement corresponds to 1/100 of a cycle of RF carrier, or about 4^{o} of sine wave. Obviously accuracies such as this require averaging of many pulses and pulse groups. Although the best signal-to-noise ratio would be achieved at the zero crossing of the third carrier cycle (see Fig. 12), the receiver must still know what cycle the time measurement is made upon, and this requires knowledge of the pulse envelope (see Section 5.2).

Initially, assume the receiver must make the time measurement in one Loran-C interval (100 ms). Then only three system pulses, one each from the master and each slave, are available. Assume we can start two counters going at the master station (we ignore the problem of identifying which of the three pulse groups is the master) and stop one counter at the first slave's first pulse and the other counter at the second slave's first pulse. The counters then indicate the t_A and t_B required. To maintain the 0.1-μs accuracy, each time measurement must be to within 0.1 μs. If the zero crossing of the third carrier cycle is used (we ignore how to determine this), its peak amplitude is about 0.45 times the peak carrier amplitude. Since the slope of the instantaneous amplitude is about unity at the zero crossing, the zero crossing must be determined to within an amplitude error of 1/100 of the third cycle amplitude. If the signal power is measured at the sampling point on the third cycle, we need at least a 40-db S/N ratio to recover the zero crossing to within 0.1 μs.

Assuming an S/N ratio of about 10 db after the gating circuitry,* we need about 30-db processing gain. If we get 3 db each time we double the (coherent) integration time, then we need about $2^{10} \simeq 1000$ basic intervals, or about 100 seconds.

5.2 Envelope

The envelope of a Loran-C pulse is represented by

$$s(t) = t^2 e^{-2t} \quad (t \geq 0)$$

to within a multiplicative constant. If this envelope is delayed by a time τ, inverted and added to s(t) with proportionality constant α, then the new signal, $s_d(t)$, is

$$s_d(t) = s(t) - \alpha\, s(t+\tau) = t^2 e^{-2t} - \alpha(t+\tau)^2 e^{-2(t+\tau)}$$

$$(t \geq 0,\ \tau \geq 0,\ \alpha > 0) \ .$$

The resulting waveform, called the derived envelope, is sketched in Fig. 13.

By choosing τ and α properly we can make the zero crossing of $e_d(t)$ occur near the sampling point at the third carrier cycle. For maximum accuracy we may also wish to adjust the constants so that the slope at the zero crossing is a maximum. Apparently this choice of

* This figure will be justified in Section 5.3.

conditions requires

$$s_d(t_s) = 0 = e^{-2t_s}\left[t_s^2 - \alpha(t_s+\tau)^2 e^{-2\tau}\right]$$

$$\frac{d}{dt} s_d(t_s) = (\max) = 2e^{-2t_s}\left[t_s(1-t_s) + \alpha e^{-2\tau}(t+\tau)(t+\tau-1)\right] ,$$

where t_s corresponds to the sampling time (3/8 for the 30-μs point discussed above). These equations can be solved for the optimized parameters α and τ, but even at the optimum values the slope of the zero crossing will be close to unity.

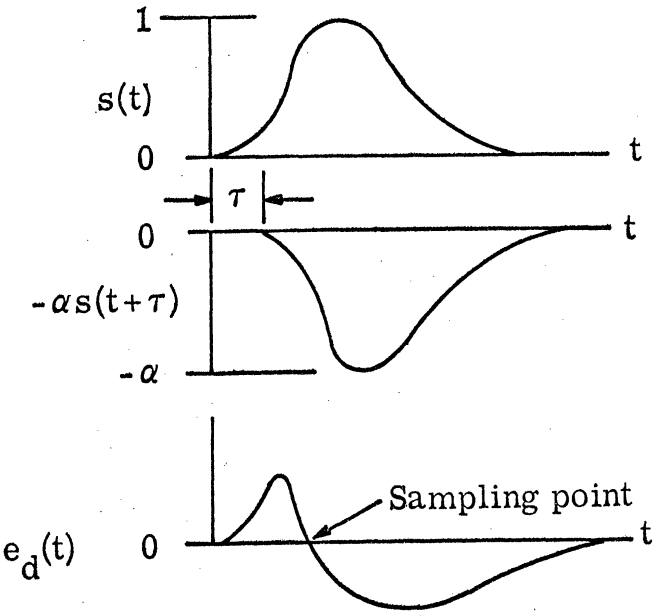

Fig. 13. Derived waveform.

If a particular carrier cycle is to be tagged without ambiguity for carrier phase, the time uncertainty must be kept within 5 μs. Since the slope of the derived envelope at the sampling point is about 1/80 μs,

we need a S/N ratio of better than $16 \simeq 24$ db. Assuming as before a preprocessing S/N ratio of 10 db, then 14 db of processing gain are required, i.e., about $2^5 = 32$ samples, or a little over 3 seconds.

5.3 Preprocessing Gating

We now have some idea of the amount of processing necessary to extract the derived envelope and the carrier phase. These processes assumed an input S/N ratio of 10 db and proper gating so that synchronous processes could be used. Now, somehow, we must perform these gating functions. We must invent a correlated integration process which will discriminate between the master and the slaves and which will elicit both from noise environments 20 db stronger than the signal. At this point we can disregard both the exact derived envelope and the carrier phase, since the objective is simply to open the proper detector gate at the proper time.

If some frivolity be allowed, we might postulate that the noise distribution following the agc-controlled stages be a loose approximation to whiganoi. This rather sleazy assumption allows some fruitful filching from the usual signal-detectability results. Since we have a signal-known-exactly-except-for-carrier-phase (and this is the crucial point), the optimum receiver for gating purposes consists of an envelope detector (either linear or square-law, depending upon the input signal-to-whiganoi ratio) followed by an integrator (low-pass filter). Filtering preceding the detector increases the postdetection S/N ratio by 3 db each time the

bandwidth is halved. Filtering following the detector increases the postdetection S/N ratio by 1.5 db each time the bandwidth is halved. Using a bandpass filter, the predetection bandwidth can be reduced to about 5 kc before the 200-μs pulses become severely distorted, and this allows a 6-db increase in postdetection S/N ratio.

But whiganoi following the agc-controlled stages is not the only problem. In the general case the differential amplitudes between the various stations may be as high as 80 db. We need a method of discriminating between a desired signal, e.g., one from the master or a slave, and the other stations of the net. Typical methods for doing this also result in some signal-to-whiganoi ratio improvement, so for the present we will ignore the influence of noise on the detection process and concentrate instead on the discrimination between the desired signal and correlated interference processes.

The gating problem presents two subproblems: First, we must identify the pulse groups as belonging to either the master or its slaves. The crosscorrelation function between the master and slave signals, calculated in Section 3.2, is important in this connection. Second, we must control the gating circuitry so that we sample the desired pulse group only when a pulse is present. This involves the autocorrelation functions of the master and the slave signals, also calculated in Section 3.2. The second problem is also complicated by skywaves; the autocorrelation functions of the Loran-C/D signals are tweaked to help eliminate the interference caused by these sources.

Implementing any of the advantages gained by signal processing and filtering involves an integration process, so we expect the correlation process to extend over at least one basic period, or about 100 ms. Also, the coding chosen for the Loran-C/D signals involves carrier-phase modulation; therefore the integration process must be coherent. We shall return to these topics in Section 6.

Having established the necessity for coherent processes in gate extraction, we shall now explore instrumentation techniques. Given a threshold detector connected to the output of the coherent integrator we probably would agree on a minimum of 10 db in S/N ratio at this point. If the signal-to-whiganoi ratio at the output of the agc-controlled stages is about unity, 10 db of coherent processing gain are required. If the signal amplitude differences reach 80 db between the stations of the triad, clearly some intelligent gating will be necessary in this process too.

We can approach this problem in two ways: Either through autocorrelation or crosscorrelation processes. The autocorrelation processes have the advantage of not requiring a locally generated synchronous signal and the tedious searching problems associated with it, while the crosscorrelation processes have the advantage of much greater S/N ratio improvements. It seems prudent in this connection to assume that, no matter what the implementation of devices to increase the ratio of desired to undesired signals, the strongest signal of the net will be captured first by linear-integration process. Once the pulse positions of this signal are

known, the intervals can be assigned a master or slave detector and gated off to the linear-integration process. In this manner, the gating circuitry peels off the time-shared signals by order of decreasing signal amplitude.

Given the estimated geographical position of the receiver, and the known position of the transmitter, one can determine the signal strengths and differential amplitudes expected at the receiver (A9). With this knowledge, one need determine only the actual time position of the composite signal relative to the local receiver clock. In this case, the intelligent receiver will not bother with crosscorrelation processes but simply autocorrelate the whole composite signal. Once the central peak of this signal has been determined in time, the proper gates can be opened for the master and slave detectors.

6. SIGNAL PROCESSING

The preceding sections have presented the Loran-C/D signal recovery process from the standpoint of maximizing signal-to-interference ratios. Throughout the discussion we have maintained the tacit assumption that some mysterious gadget was available to exchange real time for signal-to-interference ratio improvement. The last section maintained that coherent integration would be required in this process. This section will discuss various instrumentation means of realizing these procedures.

We can approach the coherent integration problem in two ways: One might be called the signal detectability approach, and involves cross-correlation techniques; the other might be called the matched filter approach, and involves autocorrelation techniques. For detecting only the presence or absence of a signal in noise the crosscorrelation techniques are considerably better than the autocorrelation techniques (D9). For determining the time-of-arrival of a signal in noise, the question is not nearly so clear cut. Each of these techniques will be discussed in succeeding sections.

6.1 Crosscorrelation Techniques

For a signal corrupted by whiganoi, the most efficient receiver is one that knows the received signal in waveshape and phase except, possibly, within a multiplicative constant of amplitude (D9). The complete receiver then has only to decide if the signal is present. The implementation of this receiver involves a device to extract the cross-

correlation function between the unknown signal-plus-noise environment and the known signal waveform. Such a device is the familiar synchronous detector, shown in Fig. 14.

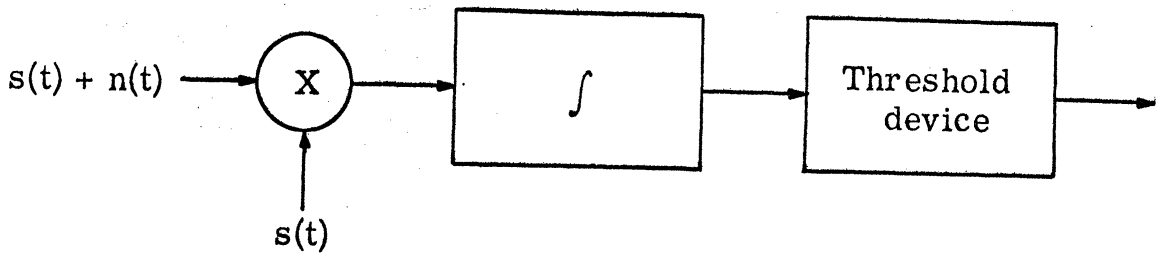

Fig. 14. Crosscorrelation detector.

In operation the integrator performs as a smoothing filter. When the output of the integrator exceeds a predetermined threshold, the threshold device notifies the outside world that the signal is present. Reference D9 discusses at great length the adjustment and parameterization of such a device.

The questions involved in evaluating this device center around the reference signal s(t) which must be generated in the receiver. Because we don't know the transmitted time position within the basic interval (indeed, that is what we try to determine), we must guess a time position and then allow the gadget to say if a signal is present. If our guess is right (a probability of 1 part in 10^6), we can announce the time-of-arrival relative to the local receiver clock; if not, we must

tediously search the entire basic interval until the signal is found.*

Briefly, the crosscorrelation detector operates as follows: Let s(t) represent a pulse of RF carrier which has been phase-flipped at clock intervals of Δt. Assume the pulse is an integral number of clock periods in length. Let s(t) be phase-flipped according to a code c(i), where $i \leq i \leq n$ and c(i) is plus or minus one according to the relative phases. We assume that the phase flips occur when the instantaneous RF amplitude is zero. We wish to extract this signal from added whiganoi and to determine its exact time of arrival relative to an arbitrary point on the waveshape.

To do this we must know the RF carrier phase and the cycle at which a transition in phase occurs. We have a local carrier and code c(i) of sufficient accuracy that integration over the entire pulse length $n\Delta t$ is practical.

One way to do this is in a synchronous detector-lowpass filter, shown in Fig. 14. We may separate the amplitude and phase information as in Fig. 15. Initially, we guess the phase of $\rho(t)$ and e(t) and examine the output of the LPF. Then we carefully search through all carrier and envelope phases until we hit upon the right one, at which time the output

* Actually in such a process some a priori information may give us a head start on a position estimate. Such a priori information may include an estimated receiver geographical position, from which all sorts of signal parameter information may be extracted such as rough time-of-arrival and differential amplitude estimates (A9).

of the LPF springs to a nice high value and the search is over.

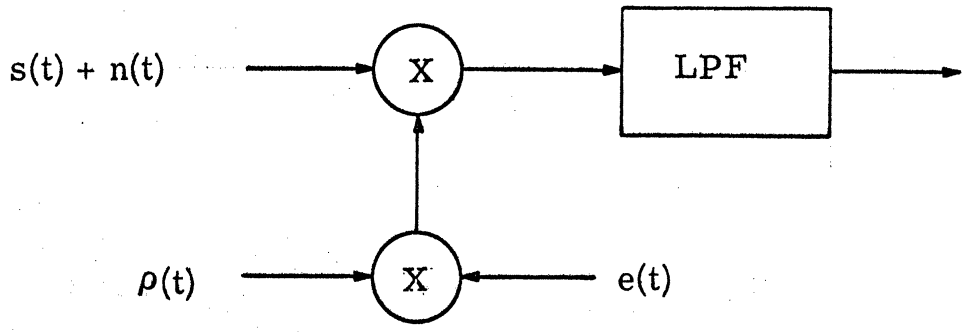

Fig. 15. Synchronous detector.

Using the commutivity of multiplication, we can rearrange the circuits, as in Fig. 16.

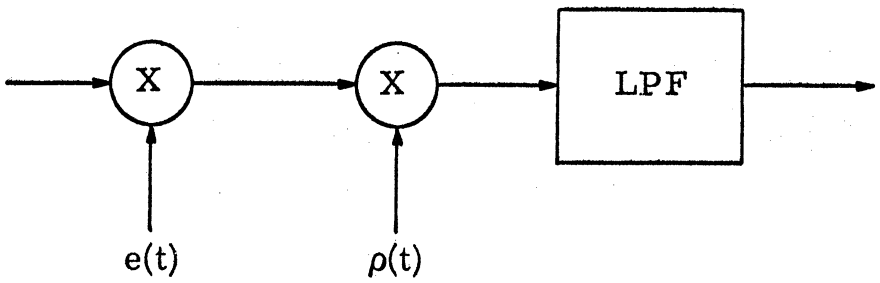

Fig. 16. Commuted synchronous detector.

Note that the signal, after passing through the first amultiplier, has been gated and "unscrambled" in phase, providing the code e(t) and the signal are in phase as to carrier envelope.

One is tempted here to put a phase-lock detector at the junction point between the two multipliers to extract the phase, and use the output to drive the second multiplier. An attractive method for deriving the carrier phase is evident.

6. 2 Autocorrelation Techniques

Let the signal at the receiver input be

$$f(t) = s(t) + n(t) \ ,$$

and assume that n(t) is a whiganoi process of spectral energy N_o watts/cycle over a band W. Also, let E be the total signal energy during a basic period T. We are interested in constructing a filter which will maximize the ratio of peak signal power to noise power. The quantity to be maximized then is

$$\rho = \frac{E}{N_o}$$

According to results from the theory of prediction and smoothing of stationary processes (D6, D7, D8), this maximum is realized at the output of a filter with transfer function proportional to

$$H(w) = S^*(\omega) \ ,$$

where $S^*(\omega)$ is the complex conjugate of the Fourier transform of s(t):

$$S(\omega) = \int_0^\infty e^{-j\omega t} s(t) \, dt \ .$$

A feeling for the kind of filter required can be realized through the impulse response (C9),

$$h(t) = \frac{1}{2\pi} \int_{-\infty}^{\infty} e^{j\omega t} H(\omega)\, dt = s(t-\tau) \quad ,$$

that is, the impulse response of the filter is just the time inverse of the signal itself. For example, if the synchronously detected Loran-C/D envelope were as in Fig. 17, then the matched filter impulse response would be as shown in Fig. 18.

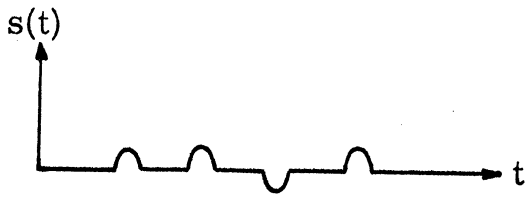

Fig. 17. Detector output.

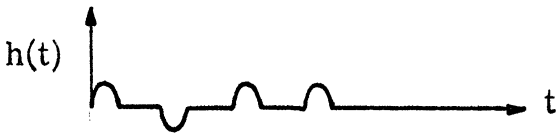

Fig. 18. Matched filter impulse response.

Since impulse responses of mortal networks must vanish for negative times, the matched filter output will be delayed by a time equal to the signal duration, which must of course be finite.

The output of the matched filter excited by s(t) alone is

$$\mu(\tau) = s(t) + h(t) = \int_{-\infty}^{\infty} s(t')\, s(t'-\tau+t)\, dt' = \psi(t-\tau) \quad .$$

In other words, the matched filter is an autocorrelator, and its response to s(t) is the autocorrelation function of s(t). Since the peak of this function occurs at $\tau = o$ and is $\psi(o) = E$, the maximum value at the output of the filter is equal to the total signal energy at the input. Then the signal-to-noise ratio is

$$\rho = \frac{E}{N_o}$$

at the filter output. We have not really gained or lost anything in total signal-to-noise powers with the matched filter but we have piled all the signal energy into one central peak in time--the peak of the autocorrelation function.

Consider the energy in a single pulse of the form $t^2 e^{-2t}$:

$$E_o = \int_{o}^{\infty} t^2 e^{-2t}\, dt = \frac{3e^4}{128} \quad .$$

The energy in the central peak of the autocorrelation function for the

16-pulse basic period will be

$$E = 16E_o = \frac{3e^4}{8} .$$

If we measure the improvement by the peak signal-to-noise ratio in the two cases, then this improvement is sixteen fold, or 12 db.

A practical matched filter for the Loran-C signal is an auto-correlator consisting of a delay line, a collection of matched subfilters, and an adder:

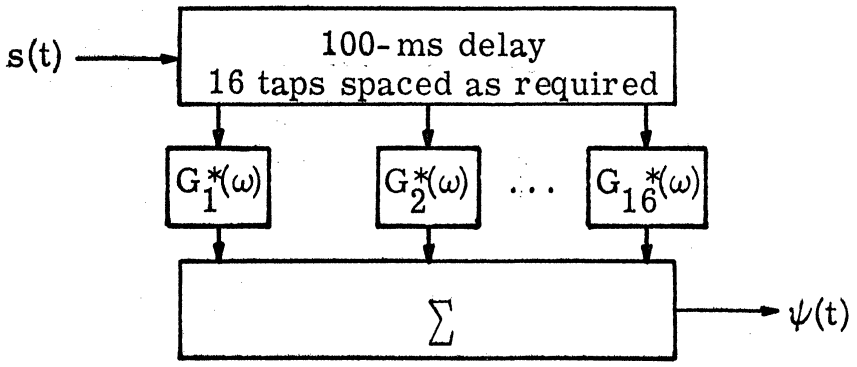

Fig. 19. Matched filter.

The 100-ms delay line has 16 taps at 1-ms intervals corresponding to the pulse positions in the transmitted code. The filters $G_1^*(\omega), \ldots, G_{16}^*(\omega)$ are matched subfilters for the corresponding phase-coded system pulses. In the Loran-C, these consist merely of inverters at the appropriate delay of the taps:* one set of inverters for the master code, and one set

* The Loran-D would have 64 subfilters.

for the slave code.

In the receiver the matched filter would precede the gating circuitry:

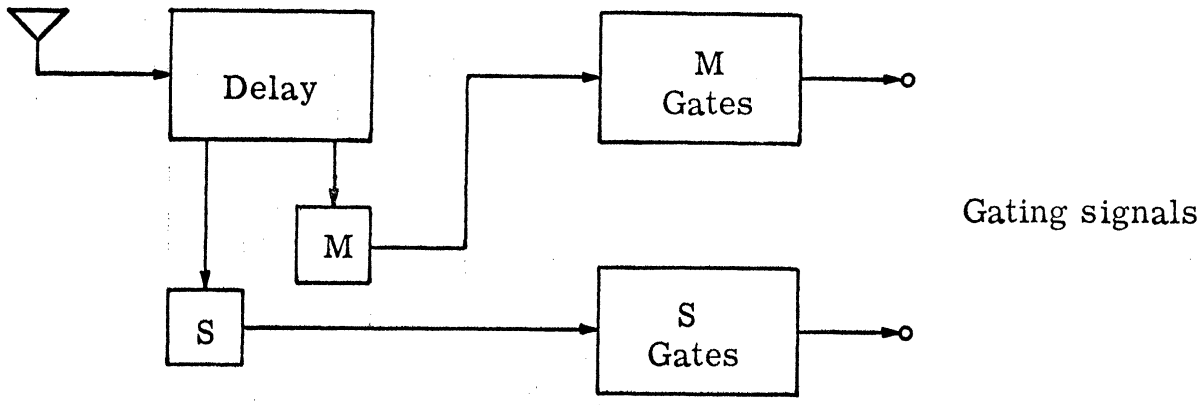

Fig. 20. Master-slave matched filters.

The boxes labeled M and S represent the inverter-adders for the master and slave codes respectively. Naturally, we are interested in the ability of this gadget to discriminate between the desired and the undesired codes, which requires the crosscorrelation between the master and the slave codes. The function is tabulated in Section 3. 2. The response of either filter to the undesired signal is the crosscorrelation function of Table 2, whereas the response of either filter to the desired signal is +16 in the same units as the Table 2. If both the master and the slave are at the same signal level, the difference between the filter outputs is only $\frac{16}{5}$ = 5 db. Undoubtedly this figure could be increased by tweaking the matched filters, but rather than design the filter for optimum whiganoi, as we have done, we should reapproach the design problem using the undesired signal as the noise process.

6.3 Comb Filters

Since the Loran-C signal as received may be immersed to noise stronger than the signal energy in the baud period, the 12 db obtained by coherent integration over the pulse group may be insufficient.

Consider for the time being that only the location of the central pulse in s(t) is desired relative to an arbitrary position in the 100-ms repetition interval. Then a postdetection S/N of +10 db appears a reasonable lower bound. If the postdetection S/N following the matched filter is less than this, the difference must be obtained by integrating over more than one pulse group.

Assume we can do this coherently. A device called a comb filter, which will realize these objectives, consists of a delay line 100-ms long in a circuit (see Fig. 19):

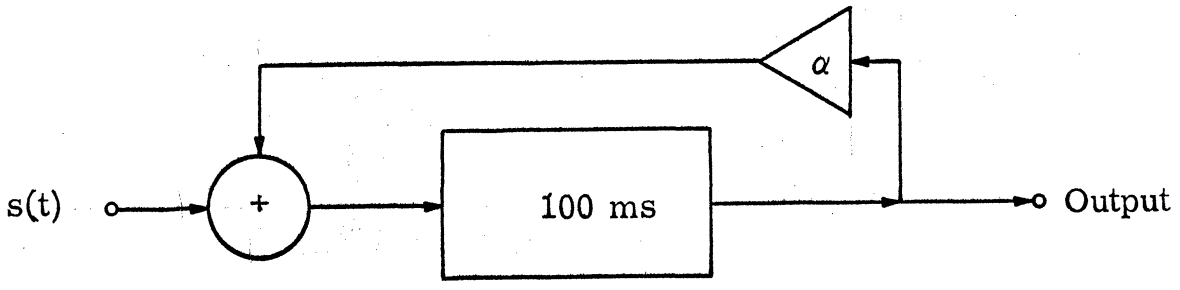

Fig. 21 Comb filter

The gain of the amplifier α is slightly less than one; how much less depends upon the bandwidth, and hence the integration time, which we shall now attempt to determine.

For each sample 100-ms period, we add E signal energy coherently and N_o noise power incoherently. That is, for each doubling of the number of samples the S/N at the output is increased by 3 db. To gain x db we need $3 \cdot 2^x$ samples, or about $t = 0.3 \cdot 10^{x/3}$ at 10 samples per second. We have assumed no decay of the "earlier" samples such as occurs in a circuit like the filter shown. We conclude that the bandwidth must be at least on the order of 1/t. We also note that the doppler must be certainly no greater than the bandwidth; this requirement limits the bandwidth to 0.2 cps for vehicle speeds less than Mach 4.

6.4 Information Storage in Integration Processes

So far, we have maintained the convenient assumption of ideal driftless integrator and delays. This section will investigate techniques of a more mortal variety.

Consider first the 100-ms delay line of the comb filter and matched filter. This component can be characterized through the sampling theorem. The delay is 100-ms, the center frequency is 100 kc, and the bandwidth is 20 kc; accordingly, a sampling rate of 2WT = 4000 samples per period will completely specify the signal process. Invoking a bit of information theory, we try to determine the precision of the samples. At the envelope detector we have determined that the S/N ratio should be greater than 24 db and the phase detector should be greater than 40 db. Choosing the latter figure, we see that the channel bit rate of the delay should be

greater than

$$H = W\log_2 \frac{S+N}{N} = 20 \times 10^3 \times 12 \cong 1 \times 10^5 \text{ bits/sec.}$$

That is, for 4000 samples per second, each sample should be coded in at least 25 bits.

We have estimated the number of samples at about 4000 per 100-ms interval. But once this interval is found, only 30 μs are of interest. Thus for only .03% of the time are the samples meaningful.

A simple code could be arranged to code the "dead time" between 200-μs correlation peaks into a single binary number. A gated memory which would recirculate the 100 or so samples actually contributing to the integration and a counter which would count down the dead time would produce an economical memory size.

These remarks assume that the envelope position has been predetermined to within some degree of confidence; this process, as we have seen, leads to a (coherent) requirement of 4000 samples. Since the envelope position information is available after only a few seconds, perhaps we can trade integration time for number of samples.

The economy of design is readily apparent. The envelope-detecting-sampling coherent integration finds the position of the central peak of r(t), after which the sample rate jumps from 10 kc to 40 kc, and the redundancy is coded out (we "match" the channel). The recirculating memory we use as a delay line requires 100-200 samples, and the circuit

changes very little between the envelope search and the phase search modes of operation.

7. BIBLIOGRAPHY

The following references represent a comprehensive bibliography of the theory and application of detection and processing techniques to pulsed systems in general and to the Loran-C/D system in particular. It is arranged to be roughly parallel to the topics discussed in this report.

The following publications were searched for pertinent papers:

Proceedings of the IEEE (formerly IRE)

IEEE Transactions on Aeronautical and Navigational Electronics

IEEE Transactions on Communications Systems

IEEE Transactions on Electronic Computers

IEEE Transactions on Information Theory

Cooley Electronics Laboratory Technical Reports.

Collateral references were found in the following publications:

Aviation Week

Electronics

IEEE Convention and Conference Records

Navigation

A collection of classical reference works is included.

A. Loran-C/D System Description

1. W. Dean, W. Frantz, and R. Frank, "A Precision Multipurpose Radio Navigation System," 1957 IRE National Convention Record, Pt. 8, pp. 79-98.

2. Radio Aids to Maritime Navigation and Hydrography--Special Publication 39, Supplementary Paper 5, Chap. 11 (Loran), International Hydrographic Bureau, Monaco, November, 1962.

3. R. L. Frank and A. H. Phillips, "Digital Loran-C Receiver Uses Microcricuits," Electronics, pp. 23-27; January 31, 1964.

4. E. Durbin, "Recent Developments in Loran-C Inertial Navigation," Navigation, Vol. 9, 2, p. 138 ff; Summer, 1962.

5. F. B. Duncan and M. C. Myers, Jr., "Technical Advances in the Loran-C System and Its Future Development, IRE Trans. on Comm. Systems, Vol. CS-3, p. 23ff; March, 1955.

6. R. L. Frank, "Multiple Pulse and Phase-Code Modulation in the Loran-C System," IRE Trans. on Aero. and Nav. Elect., Vol. ANE-7, pp. 55-61; June, 1960.

7. R. H. Doherty, et al., "Timing Potential of Loran-C," Proc. IRE, Vol. 50, pp. 53-56; January, 1962.

8. L. E. DeGroot, "Navigation and Control from Loran-C," Presented at the 20th Annual Meeting of the Institute of Navigation, June 15-17, 1964.

9. A Loran-D Navigation Set (Proposal to USAF Wright-Patterson AFB, Ohio), Engineering Proposal No. GR-5537, Instrument Division, Lear Siegler Inc., Grand Rapids, Mich; August, 1964.

10. W. Palmer, "Position Fixing by Means of Low-Frequency Ground Wave Phase," Presented at IRE National Conference on Aeronautical and Navigational Electronics, Dayton, Ohio; May, 1957.

B. VLF Propagation and Interference

1. A. D. Watt and E. L. Maxwell, "Measured Statistical Characteristics of VLF Atmospheric Radio Noise," Proc. IRE, Vol. 45, pp. 55-62; January, 1957.

2. A. D. Watt and E. L. Maxwell, "Characteristics of Atmospheric Noise from 1 to 160 Kc," Proc. IRE, Vol. 45, pp. 787-794; June, 1957.

3. J. S. Belrose, et al., "The Engineering of Communications Systems for Low Radio Frequencies," Proc. IRE, Vol. 47, pp. 661-680; May, 1959.

4. J. R. Johler, "Propagation of the Low-Frequency Radio Signal," Proc. IRE, Vol. 50, pp. 404-427; April, 1962.

5. J. R. Wait, "Introduction to the Theory of VLF Propagation," Proc. IRE, Vol. 50, pp. 1624-1647; July, 1962.

6. S. V. Chandrashekkar Aiya, "Noise Power Radiated by Tropical Thunderstorms," Proc. IRE, Vol. 43, pp. 966-974; August, 1955.

C. Pulsed-System Detection and Processing

1. B. Shepelavey, "Non-Gaussian Atmospheric Noise in Binary-Data Phase-Coherent Communication Systems," IEEE Trans. on Comm. Systems, Vol. CS-11, pp. 280-284; September, 1963.

2. J. Galejs, "Enhancement of Pulse Signals by Comb Filters," IRE Trans. on Inf. Theory, Vol. IT-4, pp. 114-124; September, 1958.

3. A. J. Mallinkrodt and T. E. Sollenberger, "Optimum Pulse-Time Determination," IRE Trans. on Inf. Theory, Vol. PGIT-3, pp. 151-159; March, 1954.

4. E. Kaufman and E. H. King, "Spectral Power Density Functions in Pulse-Time Modulation," IRE Trans. on Inf. Theory, Vol. IT-1, 1, pp. 40-46; March, 1955.

5. H. Sherman, "Some Optimal Signals for Time Measurement," IRE Trans. on Inf. Theory, Vol. IT-2, 1, pp. 24-28; March, 1956.

6. R. G. Baron, "The Vernier Time-Measurement Technique," Proc. IRE, Vol. 45, pp. 21-30; January, 1957.

7. S. G. Margolis, "The Response of a Phase-Locked Loop to a Sinusoid Plus Noise," IRE Trans. on Inf. Theory, Vol. IT-3, pp. 136-142; June, 1957.

8. R. Jaffe and E. Rechtin, "Design and Performance of Phase-Lock Circuits Capable of Near-Optimum Performance over a Wide Range of Input Signal and Noise Levels," IRE Trans. on Inf. Theory, Vol. IT-1, 1, pp. 66-76; March, 1955.

9. G. L. Turin, "An Introduction to Matched Filters, IRE Trans. on Inf. Theory, Vol. IT-6, pp. 311-329; June, 1960.

10. J. V. Harrington, "An Analysis of the Detection of Repeated Signals in Noise by Binary Integration," IRE Trans. on Inf. Theory, Vol. IT-1, 1, pp. 1-9; March, 1955.

11. D. L. Schilling, "the Response of an Automatic Phase Control System to FM Signals and Noise," Proc. IRE, Vol. 51, pp. 1306-1316; October, 1963.

12. J. A. Develet, Jr., "A Threshold Criterion for Phase-Lock Demodulation," Proc. IRE, Vol. 51, pp. 349-356; February, 1963.

13. H. A. McAleer, "A New Look at the Phase-Locked Oscillator," Proc. IRE, Vol. 47, pp. 1137-1143; June, 1959.

14. D. O. North, "An Analysis of the Factors Which Determine Signal/Noise Discrimination in Pulsed-Carrier Systems," Proc. IRE, Vol. 51, pp. 1016-1027; July, 1963.

D. General Theory of Detection in Noisy Environments

1. M. Horowitz and A. A. Johnson, "theory of Noise in a Correlation Detector," IRE Trans. on Inf. Theory, Vol. IT-1, 2, pp. 3-5; December, 1955.

2. P. Bello, "Time-Frequency Duality," IRE Trans. on Inf. Theory, Vol. IT-10, pp. 18-33; January, 1964.

3. C. E. Shannon, "Communication in the Presence of Noise," Proc. IRE, Vol. 37, pp. 10-21; January, 1949.

4. C. W. Helstrom, "The Resolution of Signals in White Gaussian Noise," Proc. IRE, Vol. 43, pp. 1111-1118; September, 1955.

5. J. P. Costas, "Poisson, Shannon, and the Radio Amateur," Proc. IRE, Vol. 47, pp. 2058-2068; December, 1959.

6. D. Middleton, An Introduction to Statistical Communication Theory, McGraw-Hill, New York, 1960.

7. Y. W. Lee, Statistical Theory of Communication, John Wiley and Sons, New York, 1960.

8. W. B. Davenport, Jr. and W. L. Root, An Introduction to the Theory of Random Signals and Noise, McGraw-Hill, New York, 1958.

9. W. W. Peterson and T. G. Birdsall, The Theory of Signal Detectability, Electronic Defense Group, Univ. of Mich., Tech-Rept. TR-13 (Parts I and II), Ann Arbor, June, 1953.